ELSEVIER

Contents lists available at ScienceDirect

Journal of Inorganic Biochemistry

journal homepage: www.elsevier.com/locate/jinorgbio





Synthesis, electronic structures, and reactivity of mononuclear and dinuclear low-valent molybdenum complexes in iminopyridine and bis (imino)pyridine ligand environments

Asanka I. Dissanayake ^a, Thilini S. Hollingsworth ^a, Sudheer S. Kurup ^a, Duleeka Wannipurage ^a, Patrick N. Hamilton ^b, Richard L. Lord ^{c,*}, Stanislav Groysman ^{a,*}

ARTICLE INFO

Keywords: Molybdenum Redox non-innocent ligands Iminopyridine Bis(imino)pyridines Bimetallics

ABSTRACT

Molybdenum in redox non-innocent ligand environments features prominently in biological inorganic systems. While Holm and coworkers, along with many other researchers, have thoroughly investigated formally highoxidation-state molybdenum (Mo(IV)-Mo(VI)) ligated by dithiolenes, less is known about molybdenum in other formal oxidation states and/or different redox-active ligand environments. This work focuses on the investigation of low-valent molybdenum in four different redox non-innocent nitrogen ligand type environments (mononucleating and dinucleating iminopyridine, mononucleating and dinucleating bis(imino)pyridine). The reaction of iminopyridine N-(2,6-diisopropylphenyl)-1-(pyridin-2-yl)methanimine (L¹) with Mo(CO)₃(NCMe)₃ produced $Mo(L^1)(CO)_3(NCMe)$. $Mo(L^1)(CO)_3(NCMe)$ undergoes transformation to $Mo(L^1)(CO)_4$ upon treatment with CS2 or prolonged stirring in dichloromethane. The reaction of the open-chain dinucleating bis(iminopyr $idine) \ \ ligand \ \ N,N'-(2,7-di-tert-butyl-9,9-dimethyl-9H-xanthene-4,5-diyl) bis (1-(pyridin-2-yl)methanimine) \ \ (L^2)$ similarly produced an hexacarbonyl complex Mo₂(L²)(CO)₆(NCMe)₂ which also underwent transformation to the octacarbonyl Mo₂(L²)(CO)₈. Both complexes featured anti-parallel geometry of the chelating units. The oxidation of Mo(L¹)(CO)₃(NCMe) with I₂ resulted in Mo(L¹)(CO)₃I₂. The reaction of mononucleating potentially tridentate bis(imino)pyridine ligand (L³) (N-mesityl-1-(6-((E)-(mesitylimino)methyl)pyridin-2-yl)methanimine) with both Mo(CO)₃(NCMe)₃ and Mo(CO)₄(NCMe)₂ produced complexes Mo(L³)(CO)₃(NCMe) and Mo(L³)(CO)₄ in which L³ was coordinated in a bidentate fashion, with one imino sidearm unbound. The reaction of dinucleating macrocyclic di(bis(imino)pyridine) analogue (L4) led to the similar chemistry of Mo₂(L4)(CO)₆(NCMe)₂ and Mo₂(L⁴)(CO)₈ complexes. Treatment of Mo(L³)(CO)₃(NCMe) with I₂ formed a mono(carbonyl) complex Mo(L³) (CO)I₂ in which molybdenum was formally oxidized and L³ underwent coordination mode change to tridentate. The electronic structures of formally Mo(0) complexes in iminopyridine and bis(imino)pyridine ligand environments were investigated by density functional theory calculations.

1. Introduction

Over the last 20 years, there has been a considerable interest in complexes of nitrogen-based redox non-innocent ligands [1–4]. Due to their ability to delocalize d-electron density and to increase the accessibility of oxidation states of the overall metal-ligand system, redox non-innocent ligands have enabled development of sustainable base-metal alternatives to precious metal catalysts [1,5]. Redox non-innocent ligands are also featured prominently in bioinorganic chemistry,

particularly in the chemistry of molybdenum (dithiolene ligation) [6,7]. Among other redox non-innocent ligands, synthetically accessible iminopyridine and bis(imino)pyridine ligands are among the most thoroughly studied. Typically, upon coordination to low-valent 3d metals (e.g. Ni(0) or Co(0)) bidentate iminopyridines can be reduced by up to two electrons [8–12], whereas tridentate bis(imino)pyridine allows an even wider range of accessible oxidation states [13–20]. However, while the electronic structures of the iminopyridine/bis(imino)pyridine 3d metal complexes have been carefully investigated, there has been significantly

E-mail addresses: patrick.hamilton@basf.com (P.N. Hamilton), lordri@gvsu.edu (R.L. Lord), groysman@chem.wayne.edu (S. Groysman).

^a Department of Chemistry, Wayne State University, 5101 Cass Ave, Detroit, MI 48202, USA

^b BASF Corporation, 1609 Biddle Ave, Wyandotte, MI 48192, USA

^c Department of Chemistry, Grand Valley State University, Allendale, MI 49401, USA

^{*} Corresponding author.

less attention to the corresponding base 4d and 5d metals, particularly molybdenum [21,22]. This is in contrast to a comprehensive investigation of molybdenum (and other 4d/5d metal) dithiolene complexes, carried out by Holm, Gray, Eisenberg, and others [23-41]. In these complexes, the redox non-innocent dithiolene ligand environment was often mixed with additional redox-active ligands including carbonyl, leading to interesting ambiguities concerning oxidation states/electronic structures of the complexes [42–47]. In contrast, studies focusing on a combination of nitrogen-based bidentate redox-active ligands (such as iminopyridines or diimines) with carbonyls at molybdenum and other heavier metals are less common. While several groups have reported the synthesis, structural characterization, and reactivity of formally Mo(0)carbonyl complexes ligated by iminopyridine ligands [48-53], investigations of the electronic structures of these complexes are rare. In recent years, the Trovitch and Chirik groups have reported synthesis and selected catalytic applications of molybdenum complexes containing tridentate bis(imino)pyridine ligands [54-61].

We have previously reported the synthesis, characterization, and reactivity of mononuclear and dinuclear nickel and cobalt complexes ligated by redox non-innocent iminopyridine and bis(imino)pyridine ligands [62,63]. It was shown that iminopyridine [NN] serves as an accumulator of redox charges for the activation of a heteroallene (carbon disulfide) mediated by nickel [64]. It was also demonstrated that bis (imino)pyridine [NNN] enables access to four different oxidation states of the metal-ligand assembly that are characterized by different coordination behavior of the ligand (most notably, bidentate vs. tridentate coordination) [65,66]. The most reduced state ({Ni[NNN]}¹⁻) led to H⁺ and CO₂ reduction [67]. Dinucleating open-chain bis(iminopyridine) ligands on a xanthene platform enabled formation of a diphenylacetylene-bridged dinickel assembly, which exhibited cooperative catalytic reactivity in cyclotrimerization [68]. A dinucleating macrocyclic di(bis(imino)pyridine) ligand formed cobalt carbonyl complexes, in which each bis(imino)pyridine chelate exhibited tridentate coordination to Co(II)/Co(I)/Co(0) centers [69]. These complexes did not exhibit reactivity with heteroallenes, and their cyclotrimerization reactivity was inferior compared to the open-chain dinickel complex. Following these studies, we became interested in an exploration of coordination chemistry and reactivity of respective complexes with the low-valent 4d metal, molybdenum. Herein we describe the coordination chemistry, electronic structure, and reactivity of mononuclear and dinuclear molybdenum-carbonyl complexes supported by mononucleating and dinucleating iminopyridine and bis (imino)pyridine complexes. The specific questions of interest in this study were: (1) What is the electronic structure (metal-ligand charge distribution) of the iminopyridine-molybdenum? (2) What is the coordination mode of the bis(imino)pyridine ligand in low-valent molybdenum complexes? (3) Given the coordination modes of mononuclear iminopyridine/bis(imino)pyridine complexes, what will be the geometry (syn or anti) and metal-metal distance of the resulting dinuclear complexes? (4) Will the mononuclear or dinuclear complexes exhibit reactivity with heteroallenes? We emphasize that nearly all molybdoenzymes feature molybdenum in redox-active (dithiolene) ligand environments. The iminopyridine ligand features similar $(0/1^-/2^-)$ redox states to the dithiolene ligand, and thus the understanding of the electronic structure of molybdenum iminopyridine complexes is of relevance to the understanding of the electronic structures of molybdoenzymes. We also note that while low-valent molybdenum bearing carbonyl ligand environments have not yet been discovered in nature, molybdenum carbonyl chemistry is of potential relevance to the reactivity of Mo-Cu carbon monoxide dehydrogenase, that catalyzes oxidation of carbonyl.

2. Experimental

2.1. General

All reactions involving air-sensitive materials were carried out in a nitrogen-filled glovebox. 2,7-Di-tert-butyl-9,9-dimethyl-4,5-diaminoxanthene, 2,6-pyridine dicarboxaldehyde, 6-(2,4,6-triisopropylphenyl)-2-pyridinecarboxaldehyde, Mo(CO)₃(NCMe)₃ (1) and Mo(CO)₄(NCMe)₂ (2) were synthesized using previously published procedures [88,89]. Carbon disulfide, phenyl isocyanate, 2,4,6-trimethyl aniline, 2-pyridine carboxaldehyde and pyridine N-oxide were purchased from Sigma and used as received. Silver hexafluorophosphate was purchased from Strem and used as received. Iodine was purchased from EMD and used as received. All non-deuterated solvents were purchased from Aldrich and were of HPLC grade. The non-deuterated solvents were purified using an MBraun solvent purification system. Dichloromethane- d_2 , benzene- d_6 and acetonitrile- d_3 were purchased from Cambridge Isotope Laboratories. All solvents were stored over 3 Å molecular sieves. Compounds were generally characterized by ¹H and ¹³C NMR spectroscopy (including 2D techniques such as ¹H—¹H COSY and HMBC), X-ray crystallography, IR spectroscopy and UV-vis spectroscopy. Satisfactory elemental analysis or high-resolution mass spectral data of the complexes examined herein could not be obtained due to oxygen sensitivity. Consequently, the complexes have been extensively characterized by NMR spectroscopy to establish bulk purity. Characterization was carried out at the Lumigen Instrument Center at Wayne State University. NMR spectra of the ligands and metal complexes were recorded on an Agilent DD2-600 MHz Spectrometer, a Varian VNMRS-500 MHz Spectrometer and an Agilent 400 MHz Spectrometer in CD₂Cl₂, C₆D₆ or CD₃CN at room temperature. Chemical shifts and coupling constants (J) were reported in parts per million (δ) and Hertz respectively. Detailed assignments of the signals in ¹H NMR are given in the ESI. UV-visible spectra were obtained on a Shimadzu UV-1800 spectrometer. IR spectra were obtained on a Shimadzu MIRacle-10 spectrometer.

2.2. Preparation of $Mo(L^1)(CO)_3(NCMe)$ (3)

A 2 mL THF solution of (E)-N-(2,6-diisopropylphenyl)-1-(pyridin-2yl)methanimine (L¹, 25.0 mg, 0.094 mmol) was added to a stirring 2 mL THF solution of Mo(CO)₃(CH₃CN)₃ (28.4 mg, 0.094 mmol). The solution color changed from yellow to blue. The reaction was stirred for 2 h, upon which the volatiles were removed in vacuo to afford 3 as a dark blue solid (44.4 mg, 0.091 mmol, 97%). X-ray quality crystals were obtained from layering of acetonitrile/ether solution at -35 °C. ¹H NMR (CD₃CN, 600 MHz) δ 9.07 (d, ${}^{3}J_{\text{HH}} = 5.3$ Hz, 1H, α -H on pyridine), 8.54 (s, 1H, imino-H), 8.04 (td, ${}^{3}J_{\text{HH}} = 7.7$, 1.3 Hz, 1H, β -H on pyridine), 7.97 (d, $^{3}J_{HH}$ = 7.6 Hz, 1H, δ-H on pyridine), 7.59 (t, $^{3}J_{HH}$ = 6.4 Hz, 1H, γ-H on pyridine), 7.27 (m, 3H, 3-H and 4-H on aniline), 3.20 (spt, $^{3}J_{HH} = 6.9$ Hz, 1H, $CH(CH_3)_2$), 3.11 (spt, ${}^3J_{HH} = 6.9$ Hz, 1H, $CH(CH_3)_2$), 1.95 (s, 3H, CH₃ on coordinated MeCN), 1.33 (d, $^{3}J_{HH} = 6.7$ Hz, 3H, CH(CH₃)₂), 1.26 (d, $^{3}J_{HH} = 6.7$ Hz, 3H, CH(CH₃)₂), 1.11 (d, $^{3}J_{HH} = 7.0$ Hz, 3H, CH(CH₃)₂), 1.06 (d, ${}^{3}J_{HH} = 6.7 \text{ Hz}$, 3H, CH(CH₃)₂) ppm; ${}^{13}C\{{}^{1}H\}$ NMR (CD₃CN, 600 MHz) δ 231.09, 229.31, 217.56, 167.80, 154.62, 152.75, 149.80, 140.51, 138.67, 129.56, 128.30, 127.59, 124.95, 124.36, 28.55, 28.25, 25.23, 23.80, 23.17 ppm. IR: $v_{C=0}$: 1898, 1782, and 1767 cm⁻¹. λ_{max} , nm ($\varepsilon_{\rm M}$, L mol⁻¹ cm⁻¹): 598 (4150), 365 (sh, 2360), 315 (sh, 4540).

2.3. Preparation of $Mo(L^1)(CO)_4$ (4)

A 2 mL THF solution of L¹ (25.5 mg, 0.096 mmol) was added to a stirring 2 mL THF solution of Mo(CO)₄(CH₃CN)₂ (27.8 mg, 0.096 mmol). The solution color changed from yellow to red-purple (magenta). The reaction was stirred for 2 h, upon which the volatiles were removed in vacuo to afford 4 as a dark red solid (46.8 mg, 0.096 mmol, 99%). ¹H NMR (CD₃CN, 600 MHz) δ 9.11 (d, ³ $J_{\text{HH}} = 5.3$ Hz, 1H, α -H on pyridine), 8.51 (s, 1H, imino-H), 8.09 (td, ³ $J_{\text{HH}} = 7.7$, 1.3 Hz, 1H, β -H on pyridine),

8.05 (d, ${}^3J_{\rm HH}=7.6$ Hz, 1H, δ-H on pyridine), 7.60 (ddd, ${}^3J_{\rm HH}=7.4$, 5.5, 1.5 Hz, 1H, γ-H on pyridine), 7.30 (m, 3H, 3-H and 4-H on aniline), 3.07 (spt, ${}^3J_{\rm HH}=6.9$ Hz, 2H, CH(CH₃)₂), 1.3 (1d, ${}^3J_{\rm HH}=6.7$ Hz, 6H, CH (CH₃)₂), 1.11 (d, ${}^3J_{\rm HH}=7.0$ Hz, 6H, CH(CH₃)₂) ppm; ${}^{13}{\rm C}\{1{\rm H}\}$ NMR (CD₃CN, 600 MHz) δ 224.55, 222.51, 204.84, 167.77, 154.46, 154.09, 148.46, 139.95, 139.09, 130.46, 128.44, 127.99, 124.96, 28.60, 25.68, 23.63 ppm. IR: v_{C=0}: 2014, 1890, 1867, and 1821 cm⁻¹. λ_{max}, nm (ε_M, L mol⁻¹ cm⁻¹): 545 (8900), 349 (sh, 5340), 301 (sh, 14,100), 285 (sh, 23,250), 261 (sh, 36,900).

2.4. Preparation of $Mo(L^1)(CO)_3I_2$ (5)

A 2 mL THF solution of I2 (12.7 mg, 0.050 mmol) was added to a stirring 2 mL THF solution of 4 (23.7 mg, 0.050 mmol). The solution color changed from red-purple to brown-purple. The reaction was stirred for 24 h, upon which the volatiles were removed in vacuo to afford 5 as a dark brown-purple solid (33.7 mg, 0.048 mmol, 96%). X-ray quality crystals were obtained from layering of dichloromethane/hexane solution at -35 °C. ¹H NMR (CD₃CN, 600 MHz) δ 9.35 (d, ³ $J_{\rm HH} = 5.6$ Hz, 1H, α -H on pyridine), 8.75 (s, 1H, imino-H), 8.26 (m, 1H, β -H on pyridine), 8.23 (t, ${}^{3}J_{HH} = 7.6$ Hz, 1H, γ -H on pyridine), 7.72 (ddd, ${}^{3}J_{HH} = 7.3$, 5.7, 1.6 Hz, 1H, para-H on aniline), 7.35 (m, 3H, meta-H and δ -H on pyridine), 2.05 (spt, ${}^{3}J_{HH} = 6.8$ Hz, 2H, $CH(CH_{3})_{2}$), 1.26 (d, ${}^{3}J_{HH} = 6.5$ Hz, 6H, CH(CH₃)₂), 1.01 (d, ${}^{3}J_{HH} = 6.7$ Hz, 6H, CH(CH₃)₂) ppm; ${}^{13}C\{{}^{1}H\}$ NMR (CD₃CN, 150 MHz) δ 171.89, 157.21, 154,08, 149.00, 141.99, 141.26, 131.46, 129.40, 129.33, 125.19, 29.58, 26.12, 22.92. ¹H NMR $(C_6D_6, 600 \text{ MHz}) \delta 8.85 \text{ (d, }^3J_{HH} = 5.3 \text{ Hz, } 1\text{H, } \alpha\text{-H on pyridine)}, 7.84 \text{ (s, }^3J_{HH} = 5.3 \text{ Hz, } 1\text{H, } \alpha\text{-H on pyridine)}$ 1H, imino-H), 7.10 (m, 3H, meta-H and para-H on aniline), 6.53 (t, ${}^3J_{\rm HH}$ = 7.3 Hz, 1H, β-H on pyridine), 6.47 (d, ${}^{3}J_{HH}$ = 7.6 Hz, 1H, δ-H on pyridine), 6.16 (t, ${}^{3}J_{HH} = 6.5 \text{ Hz}$, 1H, γ -H on pyridine), 3.62 (spt, ${}^{3}J_{HH} =$ 6.7 Hz, 2H, $CH(CH_3)_2$), 1.40 (d, $^3J_{HH} = 6.7$ Hz, 6H, $CH(CH_3)_2$), 0.99 (d, ${}^{3}J_{\rm HH} = 6.7$ Hz, 6H, CH(CH₃)₂) ppm; ${}^{13}{\rm C}\{{}^{1}{\rm H}\}$ NMR (C₆D₆, 150 MHz) δ 168.40, 155.98, 152.42, 149.23, 140.43, 139.42, 128.77, 128.38, 128.29, 128.08, 127.92, 127.09, 124.80, 29.17, 26.22, 23.34. IR: $v_{C=O}$: 2014, 1952, and 1921 cm⁻¹. λ_{max} , nm (ϵ_{M} , L mol⁻¹ cm⁻¹): 520 (5025.6), 331 (sh, 7140), 277 (sh, 15,700), 248 (sh, 33,300).

2.5. Preparation of $Mo_2(L^2)(CO)_6(NCMe)_2$ (6)

A 2 mL acetonitrile solution of (1E,1'E)-N,N'-(2,7-di-tert-butyl-9,9dimethyl-9H-xanthene-4,5-diyl)bis[1-(pyridin-2-yl)-methanimine] (L², 16.4 mg, 0.031 mmol) was added to a stirring 2 mL acetonitrile solution of Mo(CO)₃(CH₃CN)₃ (18.7 mg, 0.062 mmol). The solution color changed from pale yellow to blue. The reaction was stirred for 48 h, upon which the volatiles were removed in vacuo to afford 6 as a dark blue solid (29.8 mg, 0.031 mmol, 99%). X-ray quality crystals were obtained from a concentrated CH₃CN solution at room temperature. ¹H NMR (CD₃CN, 600 MHz) δ 8.84, (d, ${}^{3}J_{HH} = 5.3$ Hz, 2H, α -H on pyridine), 8.75 (s, 2H, imino-H), 7.70 (s, 2H, ortho-H on aniline), 7.67 (d, ${}^{3}J_{HH} =$ 2.4 Hz, 2H, δ -H on pyridine), 7.62 (t, ${}^3J_{\rm HH} = 7.7$ Hz, 2H, γ -H on pyridine), 7.55 (s, 2H, para-H on aniline), 7.23 (t, ${}^3J_{\rm HH} = 7.6$ Hz, 2H, β -H on pyridine), 1.95 (s, 3H, CH_3 on coordinated MeCN), 1.83 (s, 6H, CH_3 on xanthene), 1.41 (s, 18H, C(CH₃)₃) ppm; ¹³C{¹H} NMR (CD₃CN, 150 MHz) δ 231.05, 228.81, 218.26, 168.22, 154.69, 152.43, 146.44, 139.05, 138.36, 137.54, 130.98, 129.68, 128.19, 124.07, 122.93, 35.65, 35.18, 33.90, 31.37 ppm. IR: $v_{C=0}$: 1898, 1782, and 1767 cm⁻¹. λ_{max} , nm ($\varepsilon_{\rm M}$, L mol⁻¹ cm⁻¹): 600 (5300), 360 (sh, 6170), 312 (12580).

2.6. Preparation of $Mo_2(L^2)(CO)_8$ (7)

A 2 mL THF solution of L^2 (14.3 mg, 0.027 mmol) was added to a stirring 2 mL THF solution of Mo(CO)₄(CH₃CN)₂ (15.6 mg, 0.054 mmol). The solution color changed from yellow to red-purple (magenta). The reaction was stirred for 24 h, upon which the volatiles were removed in vacuo to afford 5 as a dark red solid (25.3 mg, 0.027 mmol, 99%). X-ray quality crystals were obtained from dichloromethane/hexane solution

at $-35\,^{\circ}$ C. 1 H NMR (CD $_{3}$ CN, 600 MHz) δ 8.92, (d, $^{3}J_{\rm HH}=5.3$ Hz, 2H, α -H on pyridine), 8.55 (s, 2H, imino-H), 7.64 (t, $^{3}J_{\rm HH}=7.6$ Hz, 2H, ortho-H on aniline), 7.60 (d, $^{3}J_{\rm HH}=2.1$ Hz, 2H, δ -H on pyridine), 7.57 (d, $^{3}J_{\rm HH}=2.3$ Hz, 2H, γ -H on Pyridine), 7.40 (d, $^{3}J_{\rm HH}=7.6$ Hz, 2H, para-H on aniline), 7.29 (t, 2H, β -H on pyridine), 1.81 (s, 6H, CH $_{3}$ on xanthene), 1.38 (s, 18H, C(CH $_{3}$) $_{3}$) ppm; 13 C{ 1 H} NMR (CD $_{3}$ CN, 150 MHz) δ 224.61, 222.12, 204.85, 202.33, 167.63, 154.02, 153.96, 146.83, 139.00, 138.91, 137.53, 131.62, 129.16, 128.31, 124.14, 122.93, 35.85, 35.22, 33.45, 31.31 ppm. IR: $v_{\rm C=O}$: 2014, 1898, 1859, and 1829 cm $^{-1}$. $\lambda_{\rm max}$, nm ($\epsilon_{\rm M}$, L mol $^{-1}$ cm $^{-1}$): 544 (13730), 388 (sh, 8750), 339 (sh, 12,930), 302 (sh, 23,150).

2.7. Preparation of $Mo(L^3)(CO)_3(NCMe)$ (8)

A 2 mL THF solution of (1E,1'E)-1,1'-(pyridine-2,6-diyl)bis(N-mesitylmethanimine) (L³,12.4 mg, 0.034 mmol) was added to a stirring 2 mL THF solution of Mo(CO)₃(CH₃CN)₃ (10.2 mg, 0.034 mmol). The solution color changed from yellow to blue. The reaction was stirred for 12 h, upon which the volatiles were removed in vacuo to afford 6 as a dark blue solid (20.3 mg, 0.034 mmol, 99%). X-ray quality crystals were obtained from a concentrated CH₃CN solution at room temperature. ¹H NMR (CD₂Cl₂, 600 MHz) δ 9.38 (br s. 1H, bound imino-H), 8.54 (br s. 2H, β-H in pyridine on bound side and unbound imino-H), 8.05 (t, ${}^3J_{\rm HH}$ = 7.6 Hz, 1H, γ-H on pyridine), 7.84 (d, $^{3}J_{HH}$ = 5.3 Hz, 1H, β-H in pyridine on unbound side), 6.98 (d, ${}^{3}J_{HH} = 14.7$ Hz, 2H, meta-H on bound aniline arm), 6.96 (d, $^3J_{\rm HH}=14.7$ Hz, 2H, meta-H on unbound aniline arm), 2.33 (br s, 3H, para-methyl on bound aniline), 2.31 (br s, 3H, paramethyl on unbound aniline), 2.26 (br s, 6H, ortho-methyl on bound aniline), 2.24 (br s, 6H, ortho-methyl on unbound aniline), 1.99 (s, 3H, H on coordinated MeCN); 1 H NMR (CD₃CN, 600 MHz) δ 9.35 (br s, 1H, bound imino-H), 8.62 (br s, 1H, β -H in pyridine on bound side), 8.52 (br s, 1H, unbound imino-H), 8.16 (t, ${}^3J_{\rm HH}=7.8$ Hz, 1H, γ -H on pyridine), 7.99 (br s, 1H, β-H in pyridine on unbound side), 6.96 (br s, 4H, meta-H on both bound and unbound aniline arms), 2.29 (br s, 6H, para-methyl on both bound and unbound aniline), 2.21 (br s, 12H, ortho-methyl on both bound and unbound aniline), 1.95 (s, 3H, CH₃ on coordinated MeCN); 13 C{ 1 H} NMR (CD₃CN, 150 MHz) δ 228.91, 218.09, 204.62, 168.98, 164.68, 164.06, 155.47, 139.46, 139.03, 131.03, 129.68, 129.61, 127.83, 127.59, 125.69, 123.61, 28.22, 20.75, 18.40, 18.26 ppm. IR: $v_{C=0}$: 1906, 1805, and 1767 cm⁻¹. λ_{max} , nm (ϵ_{M} , L mol⁻¹ cm⁻¹): 579 (3240), 366 (sh, 4840), 288 (sh, 14,170).

2.8. Preparation of $Mo(L^3)(CO)_4$ (9)

A 2 mL THF solution of L³ (13.2 mg, 0.036 mmol) was added to a stirring 2 mL THF solution of Mo(CO)₄(CH₃CN)₂ (10.4 mg, 0.036 mmol). The solution color changed from yellow to red-purple. The reaction was stirred for 24 h, upon which the volatiles were removed in vacuo to afford 9 as a red solid (20.5 mg, 0.035 mmol, 99%). X-ray quality crystals were obtained from layering of dichloromethane/hexane solution at room temperature. 1 H NMR (C₆D₆, 600 MHz) δ 9.68 (br s, 1H, bound imino-H), 8.14 (d, $^{3}J_{HH}=7.6$ Hz, 1H, β -H in pyridine on bound side), 7.23 (br s, 1H, unbound imino-H), 6.85 (br s, 2H, meta-H on bound aniline arm), 6.80 (t, ${}^3J_{\rm HH}=7.6$ Hz, 1H, γ -H on pyridine), 6.74 (br s, 2H, meta-H on unbound aniline arm), 6.53 (d, ${}^3J_{HH} = 7.0$ Hz, 1H, β-H in pyridine on unbound side), 2.36 (br s, 6H, ortho-methyl on bound aniline), 2.18 (br s, 6H, ortho-methyl on unbound aniline), 2.14 (br s, 3H, para-methyl on bound aniline), 2.12 (br s, 3H, para-methyl on unbound aniline); 1 H NMR (CD₂Cl₂, 600 MHz) δ 9.23 (br s, 1H, bound imino-H), 8.59 (br s, 1H, β -H in pyridine on bound side), 8.48 (br s, 1H, unbound imino-H), 8.12 (t, ${}^{3}J_{HH} = 7.8$ Hz, 1H, γ -H on pyridine), 7.94 (br s, 1H, β-H in pyridine on unbound side), 7.01 (br s, 2H, meta-H on bound aniline arm), 6.96 (br s, 2H, meta-H on unbound aniline arm), 2.34 (br s, 3H, para-methyl on bound aniline), 2.31 (br s, 3H, para-methyl on unbound aniline), 2.28 (br s, 6H, ortho-methyl on bound aniline), 2.23 (br s, 6H, ortho-methyl on unbound aniline); ¹³C{¹H} NMR (CD₂Cl₂, 150 MHz) δ 223.15, 222.23, 203.78, 201.60, 166.39, 162.90,157.92, 154.87, 148.89, 137.82, 136.53, 134.58, 130.33, 129.69, 129.32, 129.21, 127.99, 127.13, 125.71, 30.05, 20.89, 18.41 ppm. IR: $v_{C\equiv O}$: 2014, 1906, 1875, and 1829 cm⁻¹. λ_{max} , nm (ϵ_{M} , L mol⁻¹ cm⁻¹): 533 (6900), 374 (8350), 286 (16250), 253 (sh, 35,170).

2.9. Preparation of $Mo(L^3)(CO)I_2$ (10)

A 2 mL THF solution of I₂ (12.2 mg, 0.048 mmol) was added to a stirring 2 mL THF solution of **9** (27.8 mg, 0.048 mmol). The solution color changed from red-purple to green. The reaction was stirred for 24 h, upon which the volatiles were removed in vacuo to afford **10** as a dark green solid (35.4 mg, 0.047 mmol, 99%). X-ray quality crystals were obtained from layering of THF/ether solution at $-35\,^{\circ}\mathrm{C}$. $^{1}\mathrm{H}$ NMR (C₆D₆, 600 MHz) δ 7.22 (s, 2H, bound imino-H), 6.90 (d, $^{3}J_{\mathrm{HH}}=7.6$ Hz, 2H, β-H in pyridine), 6.82 (t, $^{3}J_{\mathrm{HH}}=7.6$ Hz, 1H, γ-H on pyridine), 6.69 (s, 2H, meta-H on aniline), 6.55 (s, 2H, meta-H on aniline), 2.64 (s, 6H, orthomethyl on aniline), 1.93 (s, 6H, orthomethyl on aniline), 1.65 (s, 6H, para-methyl on aniline); $^{13}\mathrm{C}\{^{1}\mathrm{H}\}$ NMR (CD₃CN, 150 MHz) δ 191.70, 156.64, 149.22, 140.21, 138.43, 132.66, 131.50, 130.81, 129.37, 128.29, 127.66, 121.87, 23.45, 20.97, 18.41 ppm. IR: v_{C=0}:1867 cm $^{-1}$; λ_{max} , nm (ϵ_{M} , L mol $^{-1}$ cm $^{-1}$): 518 (sh, 11,900), 439 (sh, 3030), 399 (sh, 3550), 271 (sh, 8500).

2.10. Preparation of $Mo_2(L^4)(CO)_6(NCMe)_2$ (11)

A 2 mL dichloromethane solution of (2E,5E,8E,11E)-42,47,102,107tetra-tert-butyl-49,49,109,109-tetramethyl-49H,109H-3,5,9,11-tetraaza-1,7(2,6)-dipyridina-4,10(4,5)-dixanthenacyclododecaphane-2,5,8,11-tetraene (L⁴, 15.2 mg, 0.017 mmol) was added to a stirring 2 mL dichloromethane solution of Mo(CO)₃(CH₃CN)₃ (10.2 mg, 0.034 mmol). The solution color changed from yellow to blue. The reaction was stirred for 15 min, upon which the volatiles were removed in vacuo to afford 11 as a dark blue solid (21.9. mg, 0.016 mmol, 96%). X-ray quality crystals were obtained from a concentrated CH3CN solution at -35 °C. ¹H NMR (CD₂Cl₂, 600 MHz) δ 9.67 (s, 2H, bound imino-H), 8.80 (s, 2H, unbound imino-H), 7.87 (t, ${}^3J_{\rm HH}=4.7$ Hz, 2H, γ -H on pyridine), 7.82 (d, $^3J_{\rm HH}$ = 4.4 Hz, 4H, ortho-H on bound aniline and β-H on pyridine bound side), 7.71 (d, $^3J_{\rm HH}=2.3$ Hz, 2H, para-H on bound aniline), 7.48 (d, $^3J_{\rm HH}=2.3$ Hz, 2H, β -H on pyridine unbound side), 7.44 (d, $^3J_{\rm HH}=$ 2.1 Hz, 2H, ortho-H on unbound aniline), 7.14 (d, ${}^{3}J_{HH} = 2.1$ Hz, 2H, para-H on unbound aniline), 1.91 (s, 6H, inside xanthene CH₃), 1.68 (s, 6H, outside xanthene CH₃), 1.55 (s, 6H, CH₃ on coordinated MeCN), 1.44 (s, 18H, $C(CH_3)_3$ on bound aniline), 1.31 (s, 18H, $C(CH_3)_3$ on unbound aniline) ppm.

2.11. Preparation of $Mo_2(L^4)(CO)_8$ (12)

A 2 mL THF solution of L4 (21.6 mg, 0.024 mmol) was added to a stirring 2 mL THF solution of Mo(CO)₄(CH₃CN)₂ (13.9 mg, 0.048 mmol). The solution color changed from yellow to red-purple. The reaction was stirred for 24 h, upon which the volatiles were removed in vacuo to afford 12 as a dark red solid (31.5 mg, 0.024 mmol, 99%). X-ray quality crystals were obtained from layering of THF/ether solution at −35 °C. ¹H NMR (CD₃CN, 600 MHz) δ 9.19 (s, 2H, bound imino-H), 8.83 (s, 2H, unbound imino-H), 8.02 (d, ${}^3J_{\rm HH}=7.0$ Hz, 2H, β -H on pyridine bound side), 7.99 (t, $^{3}J_{HH}$ = 7.6 Hz, 2H, γ -H on pyridine),7.80 (dd, $^{3}J_{HH}$ = 7.6, 1.4 Hz, 2H, β-H on pyridine unbound side), 7.54 (d, $^3J_{\rm HH}=2.3$ Hz, 2H, ortho-H on bound aniline), 7.47 (d, ${}^3J_{\rm HH}=2.3$ Hz, 2H, ortho-H on unbound aniline), 7.39 (d, ${}^3J_{\rm HH}=2.3$ Hz, 2H, para-H on bound aniline), 7.02 (d, ${}^{3}J_{HH} = 2.0$ Hz, 2H, para-H on unbound aniline), 1.86 (s, 6H, methyl-H on xanthene inside), 1.65 (s, 6H, methyl-H on xanthene outside), 1.39 (s, 18H, H on methyl group of t-butyl bound aniline), 1.32 (s, 18H, H on methyl group of t-butyl unbound aniline) ppm. ¹H NMR $(CD_2Cl_2, 600 \text{ MHz}) \delta 9.33 \text{ (s, 2H, bound imino-H)}, 8.80 \text{ (s, 2H, unbound means)}$ imino-H), 7.87 (m, 4H, γ-H on pyridine and β-H on pyridine unbound

side), 7.82 (d, $^3J_{\rm HH}=7.6$ Hz, 2H, β-H on pyridine bound side), 7.47 (d, $^3J_{\rm HH}=2.3$ Hz, 2H, ortho-H on bound aniline), 7.45 (d, $^3J_{\rm HH}=2.3$ Hz, 2H, ortho-H on unbound aniline), 7.42 (d, $^3J_{\rm HH}=2.1$ Hz, 2H, para-H on bound aniline), 6.95 (d, $^3J_{\rm HH}=2.3$ Hz, 2H, para-H on unbound aniline), 1.92 (s, 6H, inside CH₃ on xanthene), 1.61 (s, 6H, outside CH₃ on xanthene), 1.41 (s, 18H, C(CH₃)₃ on bound aniline), 1.31 (s, 18H, C(CH₃)₃ on unbound aniline) ppm; 13 C{ 1 H} NMR (CD₂Cl₂, 150 MHz) δ 222.61, 221.22, 203.28, 200.76, 166.50, 159.52, 157.01, 154.65, 146.68, 145.93, 142.36, 139.43, 138.57, 137.53, 137.42, 132.37, 130.97, 128.61, 124.45, 121.07, 120.66, 120.34, 114.64, 35.60, 34.68, 34.57, 34.06, 31.13, 31.05, 27.13 ppm. IR: $v_{\rm C=0}$: 2014, 1883, and 1836 cm $^{-1}$. $\lambda_{\rm max}$, nm (ε_M, L mol $^{-1}$ cm $^{-1}$): 538 (11900), 385 (20300), 339 (sh, 17,600).

2.12. Computational details

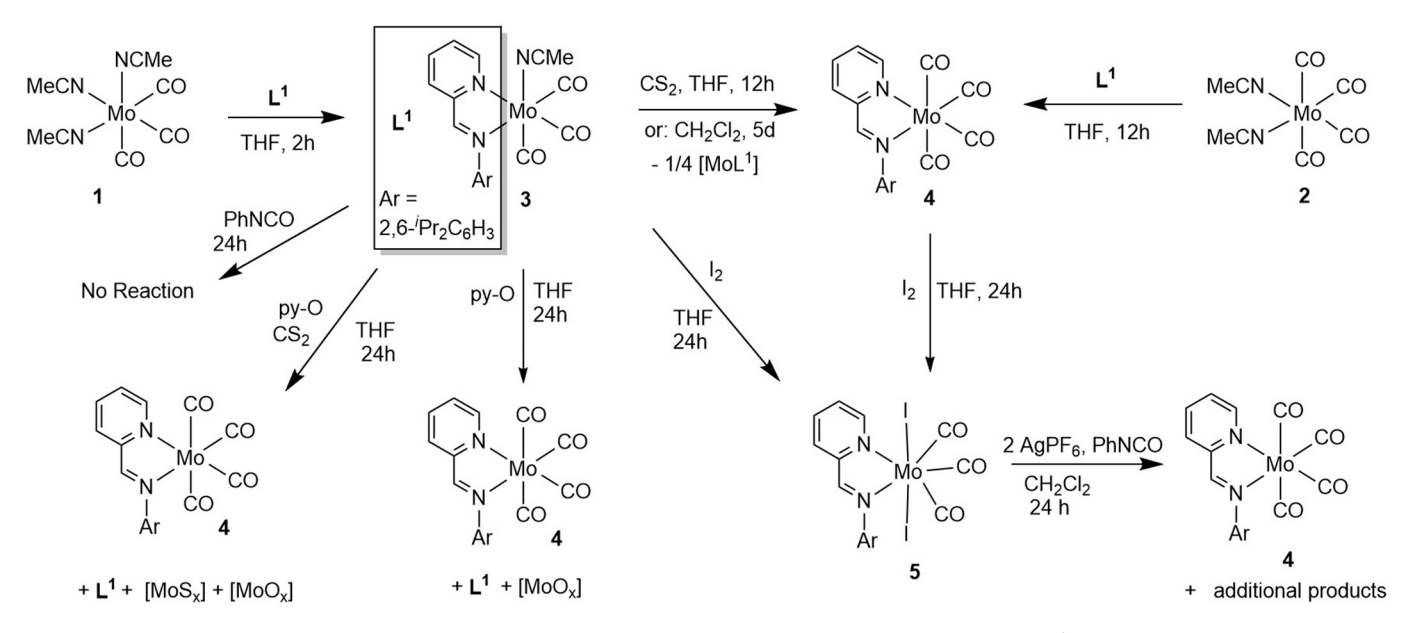
Geometry optimizations were carried out using density functional theory (DFT) at the BP86/def2-SVP level of theory as implemented in Gaussian09 (compounds that have $\rm L^3$) or Gaussian16 (compounds with $\rm L^1$) using density fitting and ultrafine grids.[70–76] Starting geometries with intraligand bond lengths corresponding to Mo(0)/L(0) and Mo(I)/L (—I) were employed with corresponding guess wavefunctions. These optimizations converged to the same structures that were confirmed to be minima based on analysis of the harmonic frequencies.[77] The final wavefunctions were confirmed to be stable.[78] UV–Vis spectra were generated by calculating the first 50 excited states using TD-CAM-B3LYP/def2-TZVP using the SMD solvation model to represent either CH₂Cl₂ or CH₃CN depending on the experimental conditions. [73,79–85].

3. Results and discussion

3.1. Synthesis and reactions of mononuclear molybdenum carbonyl complexes with mononucleating iminopyridine ligand ${\bf L}^1$

Our initial investigation focused on the reactivity of molybdenum carbonyl complexes with mononucleating iminopyridine ligand L^1 (Scheme 1). L^1 was synthesized as previously described. [86] We initially targeted a Mo(0) complex featuring at least one labile position, which could enable its subsequent reactivity with heteroallenes. Mo(CO)₃(N-CMe)₃ (1),[87,88] featuring labile NCMe ligands, was chosen as a molybdenum(0) precursor. Syntheses and reactivity of molybdenum carbonyl complexes with L^1 are presented in Scheme 1. The reaction of L^1 with 1 produced dark blue-violet complex 3 [Mo(L^1)(CO)₃(NCMe)]. 3 was characterized by L^1 H and L^1 C NMR spectroscopy, IR and UV-vis spectroscopy, and X-ray crystallography. L^1 H NMR (CD₃CN) suggested effective L^1 C symmetry in solution, containing two different L^1 Pr methine septets (3.20 and 3.11 ppm) and 4 different Me signals. The IR spectrum of 3 contained three carbonyl signals, at 1767, 1782, 1898 cm L^1 C (See Table 1.)

Treatment of 3 with carbon disulfide (CS₂) produced red-purple complex 4 [Mo(L1)(CO)4], in which the acetonitrile ligand was replaced by an additional carbonyl ligand; no incorporation of CS2 was observed. A relatively high yield of 4 (~70%) suggested the following reaction stoichiometry: $[Mo(L^1)(CO)_3(NCMe)] \rightarrow {}^{3}_{4} [Mo(L^1)(CO)_4] +$ additional products. [Mo(L¹)(CO)₄] (4) was previously reported [48], and can be obtained directly from the reaction of Mo(CO)₄(NCMe)₂ (2) and L¹. In contrast to the proton spectrum of 3, the proton spectrum of 4 is consistent with an effective C_s symmetry in solution, based on a single ⁱPr methine septet (3.07 ppm) and two methyl peaks. The IR spectrum of 4 contains 4 different CO signals, at 2014, 1890, 1867, 1821 cm⁻¹. We were not able to obtain direct evidence concerning the nature of the additional products. However, formation of dark solid was also observed in this reaction. The solid was not soluble in common organic solvents. XPS (X-ray Photoelectron Spectroscopy) analysis of the solid revealed the presence of various molybdenum sulfides (MoS2 as well as



Scheme 1. Synthesis and reactions of formally Mo(0) and Mo(II) complexes with L¹.

Table 1 Designation of compounds described in this manuscript, and their corresponding IR carbonyl stretching frequencies (cm $^{-1}$). The structures of L^1 - L^4 are provided in Schemes 1-4.

Mo(CO) ₃ (NCMe) ₃	1	1783, 1915
$Mo(CO)_4(NCMe)_2$	2	1833, 1881, 1912, 2023
$Mo(L^1)(CO)_3(NCMe)$	3	1767, 1782, 1898
$Mo(L^1)(CO)_4$	4	1821, 1867, 1890, 2014
$Mo(L^1)(CO)_3I_2$	5	1921, 1952, 2014
$Mo_2(L^2)(CO)_6(NCMe)_2$	6	1767, 1782, 1898
$Mo_2(L^2)(CO)_8$	7	1829, 1859, 1898, 2014
$Mo(L^3)(CO)_3(NCMe)$	8	1767, 1805, 1906
$Mo(L^3)(CO)_4$	9	1829, 1875, 1906, 2014
$Mo(L^3)(CO)I_2$	10	1867
$Mo_2(L^4)(CO)_6(NCMe)_2$	11	n.a. ^a
$Mo_2(L^4)(CO)_8$	12	1836, 1883, 2014

^a The complex was not isolated in a pure state and therefore its IR spectrum was not collected.

subsulfides), in addition to a small amount of molybdenum oxide, likely generated by atmospheric oxidation of the XPS sample. No reaction between $\bf 3$ and phenyl isocyanate (PhNCO) took place. $\bf 4$ did not react with either CS $_2$ or PhNCO.

The structure of **3** is provided in Fig. 1 (left); the structure of **4** was previously reported [48], and was confirmed by the unit-cell determination in this work. **3** is octahedral, demonstrating *fac* coordination of the carbonyls. The resulting C_1 symmetry in the solid state is consistent with the observed C_1 symmetry in solution. In contrast, the presence of four carbonyls in **4** leads to C_s symmetry both in the solid-state and solution. Comparison of the imine C=N bond (1.283(3) Å) and the C (imine)-C(pyridine) bond (1.458(4) Å) with the respective fully oxidized iminopyridine [8,64] indicates only small degree of iminopyridine reduction, consistent with the presence of numerous redoxactive carbonyls. The electronic structure of these complexes was further investigated by DFT (vide infra).

The UV–vis spectrum of complex 3 contains an intense peak in the visible region ($\lambda_{max}=598$ nm), in addition to two peaks in the UV region, at 365 and 315 nm (Fig. 2). Similarly, the previously reported UV–vis spectrum of 4 contains an intense peak at 545 nm, in addition to

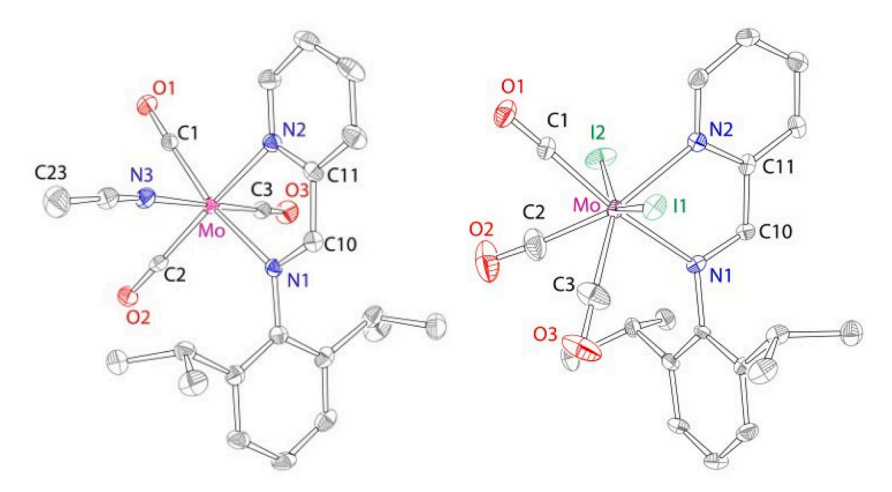


Fig. 1. X-ray structures (50% probability ellipsoids) of 3 (left) and 5 (right). Selected bond distances (Å) for 3: Mo C1 1.946(3), Mo C2 1.948(3), Mo C3 1.957, Mo N1 2.261(2), Mo N2 2.257(2), Mo N3 2.218(2), N1 C10 1.283(3), C10 C11 1.458(4). Selected bond distances (Å) for 5: Mo C1 2.01(1), Mo C2 2.00(1), Mo C3 2.00(1), Mo I1 1.839(1), Mo I2 1.827(1), Mo N1 2.23(1), Mo N2 2.22(1), N1 C10 1.29(1), C10 C11 1.45(1).

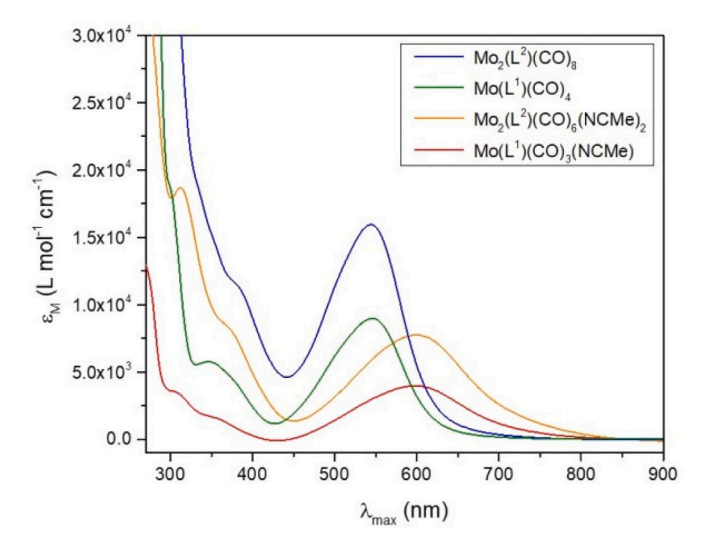


Fig. 2. The UV–Vis spectra of compounds **3** (red), **4** (green), **6** (yellow), and **7** (blue). (For interpretation of the references to color in this figure legend, the reader is referred to the web version of this article.)

several peaks in the UV (Fig. 2) [48]. The observed bathochromic shift of the corresponding λ_{max} values in the spectrum of 4 compared to 3 is responsible for the observed color differences. The computational section (vide infra) discusses the origin of these transitions.

The BP86/def2-SVP optimized structure of **3** agrees well with the experimental crystal structure (see ESI). It is important to note that no unpaired electron density at the ligand was calculated even with geometries pre-disposed toward broken-symmetry solutions. The predicted structure of **4** shows similar intraligand bond lengths of 1.314 vs. 1.321 Å, 1.446 vs. 1.442 Å, and 1.378 vs. 1.382 Å for C_{im} - N_{im} , C_{im} - C_{py} , and C_{py} - N_{py} , respectively. These values suggest comparable redoxactivity of the iminopyridine ligand in both complexes. A frontier orbital analysis of **3** shows that the HOMO (Highest Occupied Molecular Orbital), HOMO-1, and HOMO-2 are d- π in character, and the LUMO (Lowest Unoccupied Molecular Orbital) is the π^* of the iminopyridine

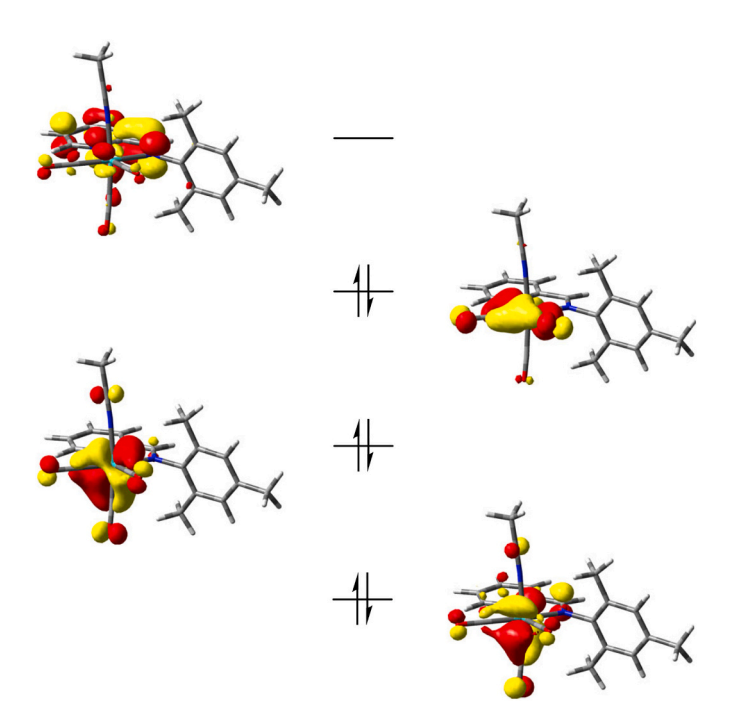


Fig. 3. Frontier orbital diagram (isosurface cutoff = 0.05 au) for 3. Orbital energy levels are qualitative and not placed on an energetic scale.

ligand (Fig. 3). There is minimal iminopyridine ligand character in the occupied orbitals, and minimal metal character in the lowest energy unoccupied orbital. A similar picture is seen for the frontier orbitals of 4 (see ESI). Based on these frontier orbitals and the intraligand bond lengths, we conclude that these species are best characterized as Mo(0) complexes similar to other Mo(0)-carbonyl species.

To better understand the bathochromic shift in the UV–Vis experiments, spectral simulations were performed at the TD-CAM-B3LYP/def2-TZVP level of theory. These simulations reproduce well the maximum low-energy absorption wavelengths of 585 and 480 nm for 3 and 4 compared to the experimentally observed values of 598 and 545 nm, respectively (Fig. 4). Unsurprisingly based on the frontier orbital diagram shown in Fig. 3, the LUMO in compounds 3 and 4 does not change much in energy from one compound to the other due to its ligand-based character. However, the highest occupied orbitals are stabilized in 4 by the additional π -backbonding of the fourth carbonyl ligand, especially in the HOMO-1 and HOMO-2 due to the axial ligand character. This creates a larger occupied/unoccupied energy gap and thus the experimentally observed bathochromic shift.

As the formally Mo(0) tricarbonyl complex 3 did not produce isolable complexes with heteroallenes, leading instead to the formation of the tetracarbonyl product 4, we investigated removal of the carbonyl ligands. Treatment of metal carbonyls (including Mo(CO)6) with an oxotransfer reagent is well known to produce CO2 and a vacant position on the metal [89-93]. The combination of 3 with pyridine N-oxide in the presence of CS2 resulted again in the formation of 4, along with free ligand L¹, in an approximately 3:1 ratio, as indicated by ¹H NMR spectroscopy. In addition, the formation of dark bluish-grey solid was observed. XPS analysis of this solid demonstrated the presence of Mo(IV) sulfide (MoS₂) and Mo suboxides/sulfides. In contrast to the previous case (a sample from the reaction of 3 with CS2), the sample also contained a significant amount of Mo(VI) oxide (MoO₃), likely resulting from oxidation by pyridine N-oxide. The reaction of 3 with pyridine Noxide produced complex 4, free ligand L¹ (both observed by NMR) and an off-white solid. The XPS characterization of this solid revealed a mixture of Mo(IV) and Mo(VI) oxides; no molybdenum sulfides were observed in this case. No reaction was observed between 4 and pyridine N-oxide. Therefore, we conclude that the oxo-transfer reagent affects oxidation of the metal instead of the carbonyl ligand.

Next, reactivity of 3 with $\rm I_2$ was investigated. Generally, Mo(II) diiodo complexes (or their zwitterionic analogues) can be generated by the combination of Mo(0) carbonyl precursors with $\rm I_2$ [94–102]. Molybdenum(II) mixed iodo carbonyl complexes with a tridentate PNP ligand have been shown to exhibit diverse structural chemistry,

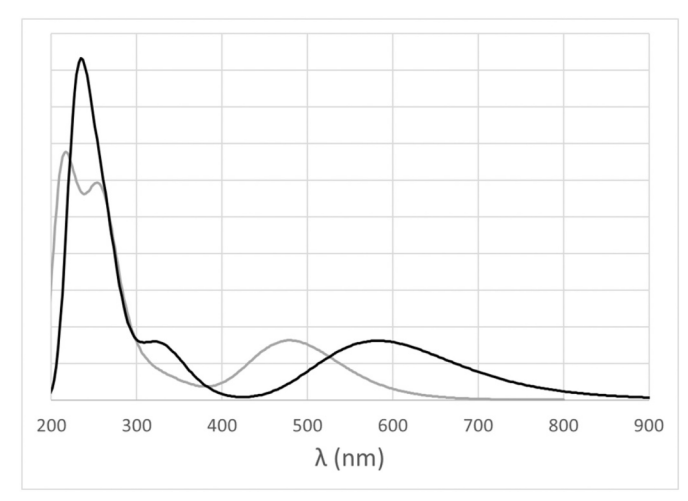


Fig. 4. Simulated UV–Vis spectra for 3 (black) and 4 (grey) at the TD-CAM-B3LYP/def2-TZVP level of theory.

including seven-coordinate [Mo{PNP}(CO)₃I]⁺ and [Mo{PNP}(CO)₂I₂], and six-coordinate [Mo{PNP}(CO)I₂] [100]. The respective Mo(II) chemistry with bidentate ligands including iminopyridine and phosphineamine ligands has been less investigated [103]. Treatment of 3 or 4 with one equivalent of iodine produced the dark purple Mo(II) complex 5. The structure of 5 was established by NMR spectroscopy and X-ray crystallography. X-ray structure determination reveals a sevencoordinate molybdenum center ligated by two approximately trans iodo groups (<I-Mo-I angle of 154.24(4) $^{\circ}$), three carbonyls in an approximately facial arrangement, and the iminopyridine ligand L¹ (Fig. 1). Similar to the Mo(0) complex 3, diagnostic iminopyridine bond distances in 5 suggest only a slight reduction of the iminopyridine ligand (for selected bond distances, see Fig. 1). The seven-coordinate, non-rigid stereochemistry of 5 is consistent with an effective C_s symmetry of the iminopyridine ligand (single type of ⁱPr substituent) in solution. The IR spectrum of 5 contains three different carbonyl peaks, at 1921, 1952, and 2014 cm⁻¹.

Treatment of **5** with AgPF₆ (slight excess) in CH₂Cl₂ in the presence of CS₂ led to a mixture of products in the ^1H NMR spectrum (light brown solution), along with the formation of a pale yellow-ash color solid. Similarly, the reaction of **5** with AgPF₆ produced a mixture of new products. Careful examination of the NMR spectra reveals similar, but not identical, products of these two reactions. Thus, one of the major products in the reaction of **5** with AgPF₆ in the absence of CS₂ appears to be a minor product in the reaction of **5** with AgPF₆/CS₂. Based on ^1H NMR analysis, none of these products appears to be the free ligand L^1 or complex **4**. In contrast, treatment of **5** with excess AgPF₆ and PhNCO produced complex **4**. Our attempts to separate these mixtures by fractional crystallization were unsuccessful.

3.2. Synthesis and structures of dinuclear molybdenum carbonyl complexes with dinucleating open-chain bis(iminopyridine) ligand L^2

We previously demonstrated that xanthene-bridged open-chain dinucleating bis(iminopyridine) ligand L^2 ($L^2 = N,N'$ -(2,7-di-tertbutyl-9,9-dimethyl-9H-xanthene-4,5-diyl)bis(1-(pyridin-2-yl)methanimine)) is capable of forming a dinickel complex in which the metals were syn and bridged by an additional ligand, acetylene [68]. Treatment of L² with two equivalents of Mo(CO)₃(NCMe)₃ in acetonitrile produced a blue-violet dinuclear complex [Mo(L²)(CO)₆(NCMe)₂] (6, Scheme 2). The X-ray structure of 6 (Fig. 5, right) demonstrates approximate (noncrystallographic) C_2 symmetry, in which the metals are positioned in an anti-parallel configuration. The xanthene linker is nearly planar (Fig. 5), as has been previously observed for di-zinc complexes with a xanthene linker in which there was no interaction between the metals [104]. In contrast, the xanthene linker was found to be bent in the di-nickel complex of L², where the metals interacted strongly via bridging alkyne ligand [68]. The molecular geometry and bond metrics at each molybdenum site are similar to those of 3. The UV-vis spectrum of 6 is also highly reminiscent of the spectrum of 3, containing peaks at 600, 360, and 312 nm (Fig. 2). The ¹H NMR spectrum of 6 demonstrates a single type of a molybdenum site, consistent with the overall C_2 symmetry of the complex, and suggesting a lack of other isomers in solution.

The combination of **6** with phenyl isocyanate exhibited no color change for 24 h; no change in the NMR spectrum was observed as well. In contrast, treatment of **6** with carbon disulfide produced red-purple $[Mo_2(L^2)(CO)_8]$ (**7**), in a transformation similar to **3** \rightarrow **4**. **7** can also be obtained by reacting L^2 with two equivalents of $Mo(CO)_4(NCMe)_2$. **7** was characterized by NMR, IR, and UV–vis spectroscopy, and X-ray crystallography. The complex features crystallographic C_2 symmetry, with two equivalent pseudo-octahedral molybdenum sites closely related to the structure of **4**. As in all previously described structures, only slight reduction of the iminopyridine is observed (for selected bond

Scheme 2. Synthesis of dinuclear complexes 6 and 7.

Scheme 3. Synthesis and reactions of molybdenum carbonyl complexes with L³.

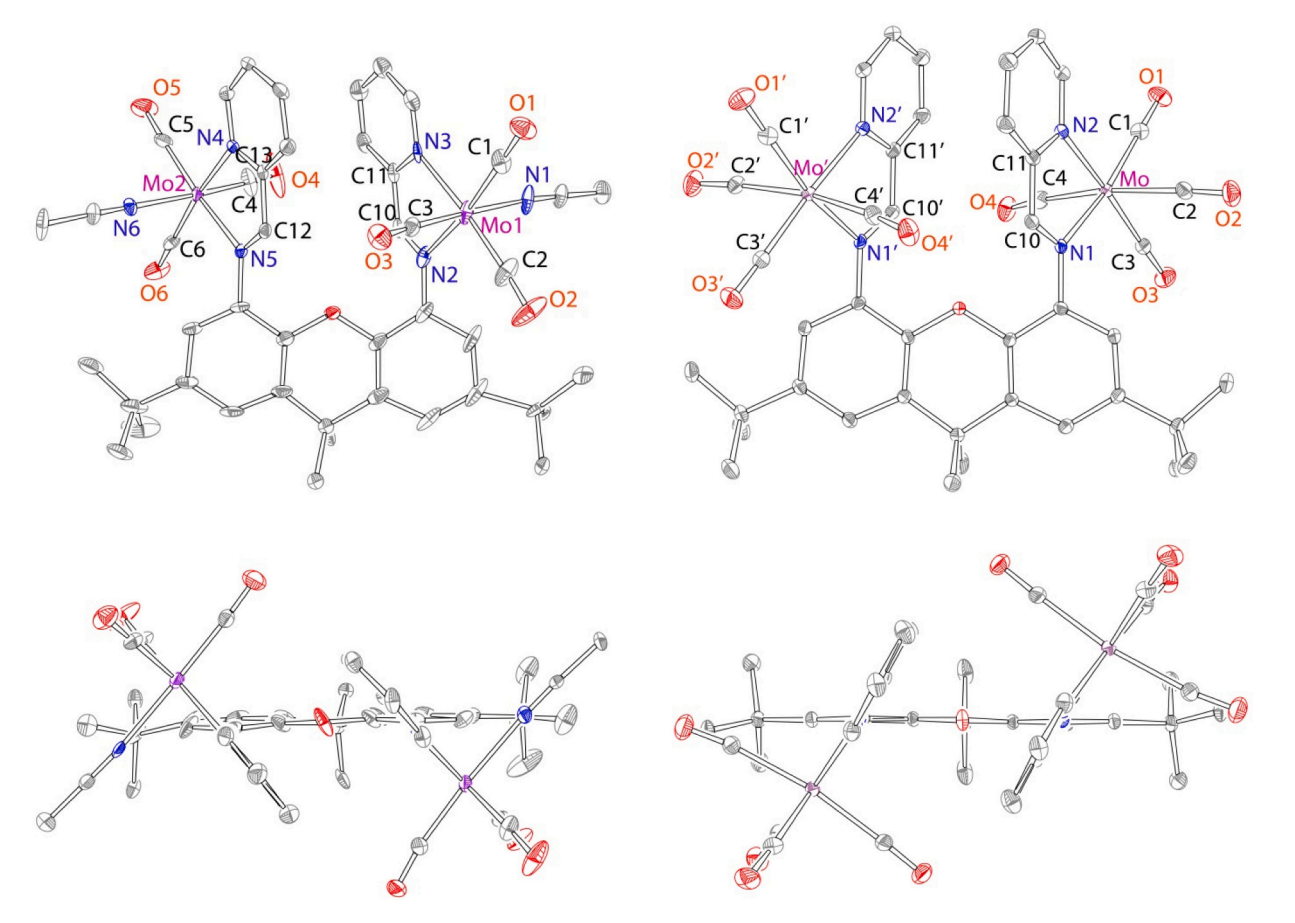


Fig. 5. X-ray structure (50% probability ellipsoids) of **6** (right) and **7** (left). Selected bond distances for **6**: Mo1 C1 1.90(1), Mo1 C2 1.94(1), Mo1 C3 1.90(1), N2 C10 1.28(1), C10 C11 1.47(1), Mo2 C4 1.94(1), Mo2 C5 1.91(1), Mo2 C6 1.94(1), N5 C12 1.29(1), C12 C13 1.43(1). Selected bond distance for **7**: Mo C1 1.964(2), Mo C2 2.060(2), Mo C3 1.970(2), Mo C4 2.024(2), N1 C10 1.285(2), C10 C11 1.456(3).

distances, see Fig. 5). Both the UV-vis and the IR spectra of 7 were very similar to the corresponding spectra of 4. Thus, 7 demonstrates a prominent peak at 544 nm (545 in 4, Fig. 2), and the IR spectrum of 7

contains four peaks attributable to carbonyl vibrations at 2014, 1898, 1859, and $1829~{\rm cm}^{-1}$, compared with signals at 2014, 1890, 1867, $1821{\rm cm}^{-1}$ for 4.

To explore whether the coordination chemistry and the relative geometry of the molybdenum sites in the complexes of L^2 can be changed, the reactivity of $\bf 6$ with $\rm I_2$ was also investigated. Treatment of $\bf 6$ with $\rm I_2$ produced brown-purple solution containing a mixture of products, according to 1H NMR spectroscopy. Based on the chemical shifts of the imine and pyridine hydrogens, this product is likely similar to $\bf 5$. The IR spectrum of the product mixture contained only two carbonyl peaks, suggesting removal of some of the carbonyl ligands via oxidation. Our attempts to further characterize these products were not successful.

3.3. Synthesis and reactions of mononuclear molybdenum carbonyl complexes with mononucleating bis(imino)pyridine ligand L³

All reactions of molybdenum carbonyl precursors with bidentate iminopyridine chelates [NN] described above led to the formation of the electronically favorable fac-[Mo(CO)3] structural unit that proved resistant to our attempts to remove a carbonyl. Thus, we turned our attention to mononucleating and dinucleating ligands featuring a tridentate bis(imino)pyridine chelate [NNN]. As the bis(imino)pyridine is expected to bind in a meridional fashion, it should lead to the formation of a mer-[Mo(CO)3] unit, which should be more amenable to removal of at least one carbonyl due to the trans effect. Stirring L³ with Mo (CO)₃(NCMe)₃ in THF or CH₂Cl₂ for a relatively short time produced dark blue 8 [Mo(L³)(CO)₃(NCMe)]. The X-ray structure of 8 (Fig. 6) revealed bidentate coordination of the potentially tridentate ligand ${\tt L}^3$ to the molybdenum center, with one imino sidearm unbound. The coordination environment at the metal is accomplished by three carbonyls and one acetonitrile ligand, resulting in a pseudo-octahedral structure similar to complex 3. While the coordinated and uncoordinated arms exhibit slight numerical differences in the C=N/C-C bond distances, relatively high esd (estimated standard deviation) values for this structure make these differences statistically insignificant. Not surprisingly, the UV-vis spectrum of 8 manifests similar features to 3. ¹H NMR spectrum (CD₂Cl₂) demonstrates a pattern consistent with two different side arms, including two different peaks for the mesityl para-methyl groups (2.33 and 2.31 ppm), and two different peaks for the mesityl ortho-methyl groups (2.26 and 2.24 ppm). Interestingly, most signals

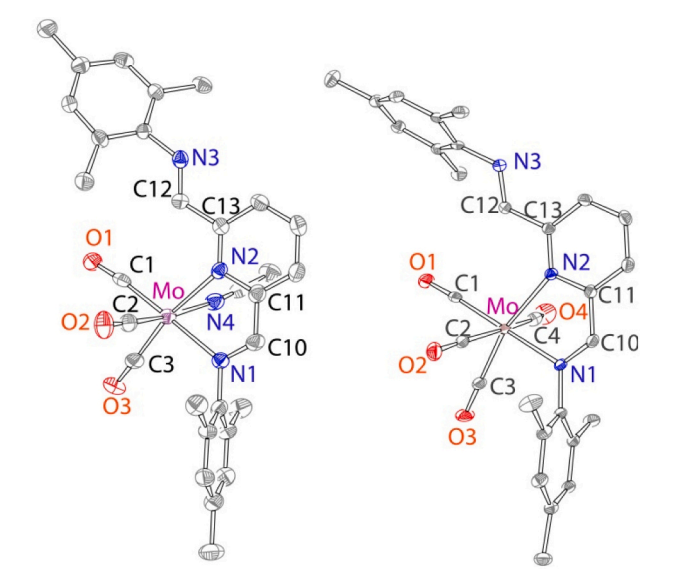


Fig. 6. X-ray structures of **8** (left) and **9** (right), 50% probability ellipsoids. Selected bond distances (Å) for **8**: Mo C1 1.946(7), Mo C2 1.947(7), Mo C3 1.935(7), Mo N1 2.232(6), Mo N2 2.327(6), Mo N4 2.216(5), N1 C10 1.278(7), C10 C11 1.456(7), N3 C12 1.268(7), C12 C13 1.470(7). Selected bond distances (Å) for **9**: Mo C1 1.965(2), Mo C2 2.036(2), Mo C3 1.956(2), Mo C4 2.039(2), Mo N1 2.219(2), Mo N2 2.324(2), N1 C10 1.279(2), C10 C11 1.454(2), N3 C12 1.268(2), C12 C13 1.480(2).

appear as broad singlets, except for the hydrogen in the 4' position of the pyridine that appears as a sharp triplet. As all the hydrogens except for this position can undergo exchange, such broadening suggests there is a relatively slow sidearm equilibration process in 8. $^{1}\mathrm{H}$ NMR spectrum taken in CD₃CN exhibits overall similar features, aside from the unresolved methyl groups that appear as two broad resonances in a 2:1 ratio. Such a finding is consistent with faster equilibration of the side arms in the coordinating acetonitrile solvent. The IR spectrum contained three carbonyl peaks at 1767, 1805, 1906 cm $^{-1}$.

Prolonged stirring of 8 (24 h) in the presence or absence of CS₂/ PhNCO (CH₂Cl₂) formed a red purple tetracarbonyl complex [Mo(L³) (CO)₄] (9), similar to what was observed with 3. The attempt to expel one of the carbonyls and transform bidentate coordination of bis(imino) pyridine to tridentate by heating 8 in toluene to 90 °C for two days [105] led to complex decomposition and the observation of the free ligand by ¹H NMR spectroscopy. **9** can be obtained directly in a nearly quantitative yield by the reaction of L³ with Mo(CO)₄(NCMe)₂. We note that the closely related complex (bearing 2,6-diisopropylphenyl-substituted bis (ketimino)pyridine) was obtained by the reaction of Mo(CO)6 and bis (imino)pyridine ligand 1,1'-(pyridine-2,6-diyl)bis(N-(2,6-diisopropylphenyl)ethan-1-imine) [106]. That reaction also produced a partially hydrogenated by-product in which one of the imino arms was transformed into amine; no additional by-products were observed in the present synthesis. 9 replicates most of the structural and spectroscopic features of 8, and the coordination environment around the molybdenum center is similar to the coordination environment of 4. ¹H NMR spectrum again suggests two different mesitylimino sidearms, containing two sets of broadened mesityl and imino resonances, while the unique 4' pyridine hydrogen gives rise to a sharp triplet. The UV-vis spectrum of 9 contains four peaks, at 533, 374, 286, and 253 nm. The structure of 9 and its selected bond metrics are provided in Fig. 6. The structure of 9 was of higher quality than 8, providing more reliable bond distances. Due to the stronger trans influence, Mo-CO bonds that are trans to each other (Mo-C2 and Mo-C4) are significantly longer than the Mo-CO bonds trans to the nitrogen donors (Mo-C1 and Mo-C3). A slight increase in the imino bond distance (N1-C10 vs. N3-C12, 1.279(2) vs. 1.268(2)) bond and the more significant decrease in the iminopyridine bond (C10-C11 vs. C12-C13, 1.454(2) vs. 1.480(2)) between the bound and the unbound arms are suggestive of some reduction of the coordinate iminopyridine arm, similar to the results described above for complexes 3-6.

Due to the potential extended conjugation provided by the second imine arm in L³ that could lower the LUMO and make L³ more redox active than L¹, 8 and 9 were optimized with BP86/def2-SVP and agree well with the experimental crystal structures (see electronic supplementary material). Despite both compounds showing signs of ligand reduction based on the experimental bond lengths, no unpaired electrons at the ligand were observed in the optimized structure of these complexes despite multiple starting geometries and electronic configurations (including broken-symmetry wavefunctions). A frontier orbital analysis of 8 shows that the three highest occupied orbitals are d- π in character, and the LUMO is the ligand π * (Fig. 7), similar to what was observed for 3. Analogous orbitals are observed for 9 (see electronic supplementary material). Based on these orbital diagrams, and the experimental and computed structural information, we conclude that these species are best characterized as Mo(0) complexes.

Treatment of red-purple 9 with I_2 in THF led to a color change to brown. Filtration and recrystallization of the crude product yielded green-brown 10. 10 was characterized by X-ray crystallography and 1 H NMR, UV–vis, and IR spectroscopy. In contrast to all previous complexes, the IR spectrum demonstrated a single carbonyl stretch at 1867 cm $^{-1}$. X-ray crystallography reveals formally molybdenum(II) octahedral complex in which the previously bidentate bis(imino)pyridine ligand L^3 now binds in a tridentate fashion, with one iodide *trans* to pyridine and the other iodide *trans* to carbonyl (Fig. 8). In addition to the three nitrogen donors of L^3 , the molybdenum center is surrounded by

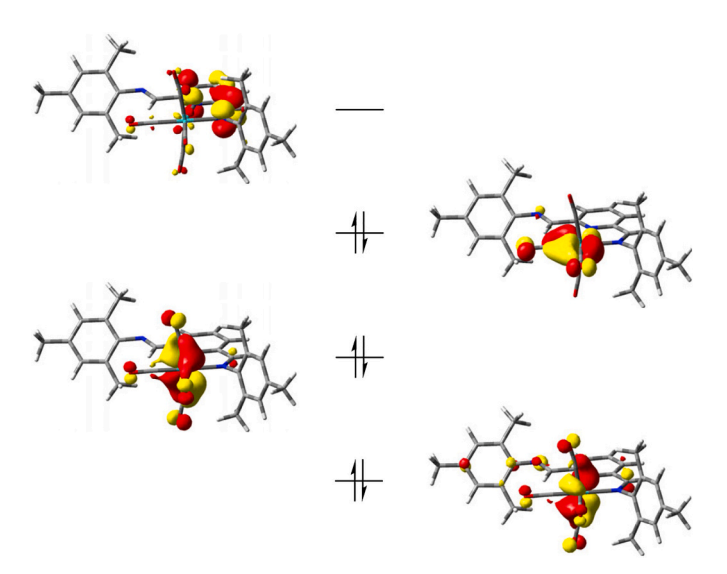


Fig. 7. Frontier orbital diagram (isosurface cutoff = 0.05 au) for 8. Orbital energy levels are qualitative and not placed on an energetic scale.

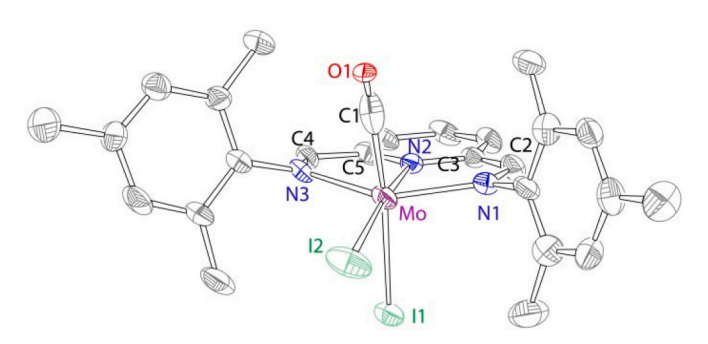


Fig. 8. X-ray structures of **10**, 50% probability ellipsoids. Selected bond distances (Å): Mo I1 2.864(1), Mo I2 2.684(1), Mo C1 2.07(1), Mo N1 2.13(1), Mo N2 2.11(1), Mo N3 2.13(1), N1 C2 1.30(1), C2 C3 1.40(1), N3 C4 1.30(1), C4 C5 1.42(1).

two iodides and a single carbonyl ligand, consistent with a single carbonyl stretch in IR. The rigid octahedral structure of **10** in solution featuring tridentate binding of L³ is further supported by NMR spectroscopy. Unlike **8** or **9**, **10** gives rise to sharp peaks suggesting the lack of a dynamic process. Additionally, the pyridine ring now gives rise to two signals: 3' protons appear as one doublet, and the 4' proton appears as a triplet. Different chemical environments below and above the [NNN] plane result in three different peaks for the mesityl methyls, and two different peaks for the mesityl aryl protons.

We also investigated the reactivity of complex ${\bf 10}$ with AgPF₆ in the presence or absence of CS₂. Treatment of ${\bf 10}$ with AgPF₆ in the presence of CS₂ formed green-brown solution and pale yellow-ash color solid. The $^1{\rm H}$ NMR spectrum of the soluble phase (CD₃CN) suggested formation of a mixture of compounds. The reaction of ${\bf 10}$ with AgPF₆ in the absence of CS₂ produced yellow-brown solution and pale yellow-ash color solid. The $^1{\rm H}$ NMR of the product was very similar to the NMR spectrum of the reaction with CS₂, suggesting that CS₂ does not participate in the reaction. In both cases, the products were not soluble in the low-polarity solvent (C₆D₆). Based on the above, we postulate that the reaction produces ionic complexes incorporating acetonitrile, [Mo(L³)(CO)(I)_{2-n}(NCMe)_n].

3.4. Synthesis of dinuclear molybdenum carbonyl complexes with dinucleating di(bis(imino)pyridine) ligand L^4

We previously reported synthesis and reactivity of macrocyclic xanthene-bridged di(bis(imino)pyridine) L⁴ with a cobalt(0) carbonyl precursor, Co₂(CO)₈ [69]. This "double-decker" ligand was found to lead to dinuclear/tetranuclear cobalt carbonyl complexes in which each of the bis(imino)pyridine chelates invariably demonstrated tridentate coordination (Scheme 4). Related macrocyclic di(bis(imino)pyridine) ligands also generally demonstrate tridentate coordination with 3d metals, including Fe, Co, Ni, and Zn [107–110]. Treatment of L⁴ with Mo (CO)₃(NCMe)₃ (1) in CH₂Cl₂ formed blue-violet dinuclear complex [Mo₂(L⁴)(CO)₆(NCMe)₂] 11, which was identified by ¹H NMR spectroscopy and X-ray crystallography (co-crystallized with 12, Scheme 5 and Fig. 9). Although at short reaction times (~15 min) a relatively clean proton NMR of complex 11 can be obtained, it is unstable in solution and converts to red-purple complex 12. 11 and 12 constitute dinuclear analogues of complexes 8 and 9, and the reaction is likely to proceed via a similar route.

The X-ray structures of complexes 11 and 12 are presented in Fig. 9. Our attempts to crystallize freshly prepared 11 led to a crystal structure containing both 11 and 12 in the asymmetric unit (11/12, Fig. 7). Pure 12, however, can be crystallized separately from 11; its independent structure is provided in the supporting information. The solid-state structure of 12 from 11/12, and independent 12, demonstrate similar structural parameters. Despite the potentially tridentate rigid chelating site that has been previously demonstrated to coordinate metal carbonyl in a tridentate fashion (Scheme 4), L⁴ in all cases coordinates molybdenum in a bidentate (iminopyridine) fashion, with one of the imines unbound. Due to the anti relative disposition of the pyridine nitrogen and the unbound imine nitrogen, the xanthenes are further apart from each other compared with the complexes where both imines were coordinated to the metal [69]. There is a wider angle between the iminopyridine chelate planes (Mo[NCCN]) in 11 (47°) vs. 12 (33° in both structures), likely because of the presence of bulkier acetonitrile ligands between the planes. Due to the same reason, the chelating iminopyridines occupy alternating positions in each complex, thereby positioning the [Mo(CO)₃(NCMe)]/[Mo(CO)₄] fragments not directly on top of each other, and leading to the (non-crystallographic) C_2 symmetry for both complexes. Metal coordination environments in complexes 11 and 12 are closely related to the coordination environments in 3 and 4, 6 and 7, and 8 and 9, respectively. Bond metrics in both structures follow the same trends discussed above for the structures of 3 and 4, 6 and 7, and 8 and 9.

 1 H NMR of free L 4 is consistent with a "bowl" structure of C_{2v} symmetry, containing four identical tert-butyl groups, two different methyl groups ("in" and "out"), two different resonances for the xanthene aryl protons, and a single resonance for the four imino hydrogens [69]. In contrast, the spectrum of pure 12 suggests effective C_{2} symmetry in solution, consistent with the solid-state structure. The spectrum contains two different tert-butyl groups, two different methyl groups, and two different imine hydrogens. Significantly, the xanthene aryl protons appear as four doublets. As only the transient spectrum of 11 was obtained, it will not be discussed in details. The attempted reactivity studies of 12 with 1_{2} failed to result in an isolable product, and the reaction of transient 11 with CS_{2} led mostly to the formation of complex 12

4. Summary and conclusions

We have conducted a comprehensive investigation of the reactivity of Mo(0) carbonyl precursors $Mo(CO)_3(NCMe)_3$ and $Mo(CO)_4(NCMe)_2$ with mononucleating and dinucleating iminopyridine and bis(imino) pyridine ligands. The products of the reactions were characterized by X-ray crystallography, NMR spectroscopy, UV–vis spectroscopy, and IR spectroscopy. Invariably, the reactions were found to lead to the

Scheme 4. Reactivity of L⁴ with Co₂(CO)₈.

Scheme 5. Formation of dinuclear molybdenum carbonyl complexes 11 and 12.

bidentate coordination of both iminopyridine and bis(imino)pyridine ligand to the formally Mo(0) center to produce Mo[κ^2 -NN](CO)₃(N-CMe). The electronic structure of this persistent structural motif was investigated by DFT calculations. In all cases the complexes were best characterized as Mo(0), based on inspection of the frontier orbitals that were highly localized. Thus, in contrast to the behavior of the low-valent 3d metals, which typically exhibit substantial delocalization of the reducing equivalents into the redox-active iminopyridine/bis(imino) pyridine framework, the corresponding low-valent 4d metal retains a "classical" $[Mo(CO)_n]^0$ /neutral [NN] ligand electron distribution. It is noted that the π -acidic (carbonyl) ligands undoubtedly accept some of the electron density from Mo(0). However, the corresponding 3d metals bearing both iminopyridine/bis(imino)pyridine and π -acidic ligands usually display substantial transfer of reducing equivalents into the redox-active ligand framework [1-5]. We also note that redox noninnocence of Mo was demonstrated in other ligand systems, bearing a

formally high-oxidation state metal [111-113].

Upon treatment with selected heteroallenes (CS₂, PhNCO), or upon prolonged stirring in solution, $Mo[\kappa^2\text{-NN}](CO)_3(NCMe)$ was found to transform into another persistent "Mo(0)" motif, $Mo[\kappa^2\text{-NN}](CO)_4$, for both iminopyridines and bis(imino)pyridines. No formation of putative "Mo[NNN]*mer*-(CO)₃ occurred upon various forcing reaction conditions. Similar molybdenum carbonyl chemistry was observed with dinucleating xanthene-bridged open-chain bis(iminopyridine) and macrocyclic di (bis(imino)pyridine) ligands. While the relative geometry of the molybdenum centers for the different dinuclear species was different, no interaction between the metals in either case was observed. Treatment of the molybdenum carbonyl complexes with an oxo-transfer agent did not result in the oxidation of CO, but oxidized the metal instead. The combination of formally Mo(0) carbonyl precursors with I_2 affected their oxidation, producing formally Mo(II) complexes. For I_2 , the paths of iminopyridine and bis(imino)pyridine complexes diverged. In the

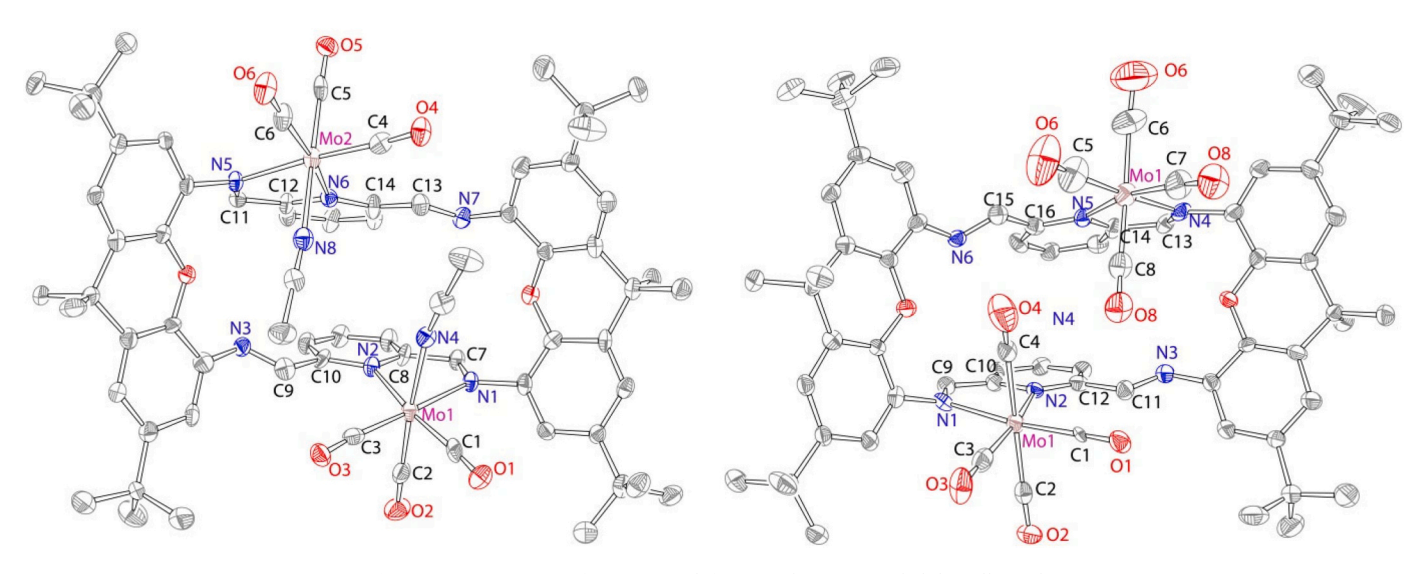


Fig. 9. X-ray structure of 11/12 (11, left, 12, right). 50% probability ellipsoids.

case of the iminopyridine ligand, the oxidation of Mo[NN](CO)₃(NCMe) (3) or Mo[NN](CO)₄ (4) leads to the formation of 7-coordinate tri-carbonyl Mo[NN](CO)₃I₂ (5). In contrast, treatment of the corresponding bis(imino)pyridine precursors Mo[NNN](CO)₃(NCMe) (8) or Mo[NNN] (CO)₄ (9) with I₂ leads to the formation of a 6-coordinate mono-carbonyl complex Mo[NNN](CO)I₂ (10). While all Mo-iodo complexes undergo reactions with Ag^+ , these reactions failed to form isolable products.

Author Statement

All authors contributed to planning, executing research activities and preparing the manuscript for publication.

Declaration of Competing Interest

No conflicts of interest to declare.

Acknowledgements

This manuscript is dedicated to the memory of Prof. R. H. Holm. We are grateful to BASF corporation for their current support. Experimental characterization was carried out at Lumigen Instrument Center of Wayne State University. Asanka I. Dissanayake is a Rumble Fellow.

Appendix A. Supplementary data

Supplementary data to this article can be found online at https://doi.org/10.1016/j.jinorgbio.2022.111744.

References

- P.J. Chirik, K. Wieghardt, Radical ligands confer nobility on base-metal catalysts, Science 327 (2010) 794–795, https://doi.org/10.1126/science.1183281.
- [2] K.G. Caulton, Systematics and future projections concerning redox-noninnocent amide/imine ligands, Eur. J. Inorg. Chem. 2012 (2012) 435–443, https://doi. org/10.1002/ejic.201100623.
- [3] L.A. Berben, Catalysis by aluminum(III) complexes of non-innocent ligands, Chem. Eur. J. 21 (2015) 2734–2742, https://doi.org/10.1002/chem.201405400.
- [4] Q. Knijnenburg, S. Gambarotta, P.H.M. Budzelaar, Ligand-centred reactivity in diiminepyridine complexes, Dalton Trans. 46 (2006) 5442–5448, https://doi. org/10.1039/B612251E.
- [5] V. Lyaskovskyy, B. de Bruin, Redox non-innocent ligands: versatile new tools to control catalytic reactions, ACS Catal. 2 (2012) 270–279, https://doi.org/ 10.1021/cs200660v
- [6] J. McMaster, C.D. Garner, E.I. Stiefel, Molybdenum enzymes, in: I. Bertini, H. B. Gray, E.I. Stiefel, J.S. Valentine (Eds.), Biological Inorganic Chemistry: Structure and Reactivity, University Science Books, Sausalito, CA, 2007, pp. 518–545.

- [7] M.L. Kirk, R.L. McNaughton, M.E. Helton, The electronic structure and spectroscopy of metallo-dithiolene complexes, in: E.I. Stiefel (Ed.), Dithiolene Chemistry vol. 52, John Wiley and Sons, Inc, New York, NY, 2004, pp. 111–212.
- [8] C.C. Lu, E. Bill, T. Weyhermüller, E. Bothe, K. Wieghardt, Neutral bis (α-iminopyridine) metal complexes of the first-row transition ions (Cr, Mn, Fe, Co, Ni, Zn) and their monocationic analogues: mixed valency involving a redox noninnocent ligand system, J. Am. Chem. Soc. 130 (2008) 3181–3197, https:// doi.org/10.1021/ja/10663n.
- [9] C.C. Lu, T. Weyhermüeller, E. Bill, K. Wieghardt, Accessing the different redox states of α-iminopyridines within cobalt complexes, Inorg. Chem. 48 (2009) 6055–6064, https://doi.org/10.1021/ic9004328.
- [10] H.P. Nayek, N. Arleth, I. Trapp, M. Loeble, P. Ona-Burgos, M. Kuzdrowska, Y. Lan, A.K. Powell, F. Breher, P.W. Roesky, Sodium and potassium Ssalts of mono- and dianionic α-iminopyridines, Chem. Eur. J. 17 (2011) 10814–10819, https://doi. org/10.1002/chem.201101646.
- [11] A.M. McDaniel, H.-W. Tseng, E.A. Hill, N.H. Damrauer, A.K. Rappe, M.P. Shores, Syntheses and photophysical investigations of Cr(III) hexadentate iminopyridine complexes and their tris(bidentate) analogues, Inorg. Chem. 52 (2013) 1368–1378, https://doi.org/10.1021/ic302055r.
- [12] K. Kowolik, M. Shanmugam, T.W. Myers, C.D. Cates, L.A. Berben, A redox series of gallium(III) complexes: ligand-based two-electron oxidation affords a gallium-thiolate complex, Dalton Trans. 41 (2012) 7969–7976, https://doi.org/ 10.1039/C2DT301124
- [13] S.C. Bart, K. Chlopek, E. Bill, M.W. Bouwkamp, E. Lobkovsky, F. Neese, K. Wieghardt, P.J. Chirik, Electronic structure of bis(imino)pyridine iron dichloride, monochloride, and neutral ligand complexes: a combined structural, spectroscopic, and computational study, J. Am. Chem. Soc. 128 (2006) 13901–13912, https://doi.org/10.1021/ja064557b.
- [14] S.C. Bart, E. Lobkovsky, E. Bill, K. Weighardt, P.J. Chirik, Neutral-ligand complexes of bis(imino)pyridine iron: synthesis, structure, and spectroscopy, Inorg. Chem. 46 (2007) 7055–7063, https://doi.org/10.1021/ic700869h.
- [15] B.M. Wile, R.J. Trovitch, S.C. Bart, A.M. Tondreau, E. Lobkovsky, C. Milsmann, E. Bill, K. Wieghardt, P.J. Chirik, Reduction chemistry of aryl- and alkyl-substituted bis(imino)pyridine iron dihalide compounds: molecular and electronic structures of [(PD)2Fe] derivatives, Inorg. Chem. 48 (2009) 4190–4200, https://doi.org/10.1021/ic801623m.
- [16] A.C. Bowman, C. Milsmann, C.C.H. Atienza, E. Lobkovsky, K. Wieghardt, P. J. Chirik, Synthesis and molecular and electronic structures of reduced bis(imino) pyridine cobalt dinitrogen complexes: ligand versus metal reduction, J. Am. Chem. Soc. 132 (2010) 1676–1684, https://doi.org/10.1021/ja908955t.
- [17] I. Vidyaratne, I. Scott, S. Gambarotta, P.H.M. Budzelaar, Dinitrogen activation, partial reduction, and formation of coordinated imide promoted by a chromium diiminepyridine complex, Inorg. Chem. 46 (2007) 7040–7049, https://doi.org/10.1021/jc70810f
- [18] T.D. Manuel, J.-U. Rohde, Reaction of a redox-active ligand complex of nickel with dioxygen probes ligand-radical character, J. Am. Chem. Soc. 131 (2009) 15582–15583, https://doi.org/10.1021/ja9065943.
- [19] D. Zhu, I. Thapa, I. Korobkov, S. Gambarotta, P.H.M. Budzelaar, Redox-active ligands and organic radical chemistry, Inorg. Chem. 50 (2011) 9879–9887, https://doi.org/10.1021/ic2002145.
- [20] A.M. Tondreau, S.C.E. Stieber, C. Milsmann, E. Lobkovsky, T. Weyhermüller, S. Semproni, P.J. Chirik, Oxidation and reduction of bis (imino) pyridine iron dinitrogen complexes: evidence for formation of a chelate trianion, Inorg. Chem. 52 (2013) 635–646. https://doi.org/10.1021/jc301675t.
- [21] G.W. Margulieux, M.J. Bezdek, Z.R. Turner, P.J. Chirik, Ammonia activation, H2 evolution and nitride formation from a molybdenum complex with a chemically and redox noninnocent ligand, J. Am. Chem. Soc. 139 (2017) 6110–6113, https://doi.org/10.1021/jacs.7b03070.

- [22] R. Pal, J.A. Laureanti, T.L. Groy, A.K. Jones, R.J. Trovitch, Hydrogen production from water using a bis(imino)pyridine molybdenum electrocatalyst, Chem. Commun. 52 (2016) 11555–11558, https://doi.org/10.1039/C6CC04946J.
- [23] R. Eisenberg, H.B. Gray, Noninnocence in metal complexes: a dithiolene dawn, Inorg. Chem. 50 (2011) 9741–9751, https://doi.org/10.1021/ic2011748.
- [24] H.B. Gray, R. Williams, I. Bernal, E. Billig, A spin-free square planar cobaltous complex, J. Am. Chem. Soc. 84 (1962) 3596–3597, https://doi.org/10.1021/ ia00877a045.
- [25] H.B. Gray, E. Billig, The electronic structures of square-planar metal complexes. III. High-spin planar cobalt(I) and iron(I), J. Am. Chem. Soc. 85 (1963) 2019–2020, https://doi.org/10.1021/ja00896a028.
- [26] A. Davison, N. Edelstein, R.H. Holm, A.H. Maki, Further examples of complexes related by electron-transfer reactions: complexes derived from bis (trifluoromethyl)-1,2-dithietene, Inorg. Chem. 3 (1964) 814–823, https://doi.org/ 10.1021/ic50016a007.
- [27] A. Davison, N. Edelstein, R.H. Holm, A.H. Maki, Synthetic and electron spin resonance studies of six-coordinate complexes related by electron-transfer reactions, J. Am. Chem. Soc. 86 (1964) 2799–2805, https://doi.org/10.1021/ ia01068a010.
- [28] A. Davison, N. Edelstein, R.H. Holm, A.H. Maki, Electron paramagnetic resonance studies of the electronic structures of bis(maleonitriledithiolato)copper(II), -nickel(III), -cobalt(II), and -rhodium(II) complexes, J. Am. Chem. Soc. 86 (1964) 4580–4587, https://doi.org/10.1021/ja01075a013.
- [29] A. Davison, N. Edelstein, R.H. Holm, A.H. Maki, The preparation and characterization of four-coordinate complexes related by electron-transfer reactions, Inorg. Chem. 2 (1963) 1227–1232, https://doi.org/10.1021/ ic50010a031.
- [30] R. Eisenberg, J.A. Ibers, Trigonal-prismatic coordination: the crystal and molecular structure of tris(cis-l,2-diphenylethene-l,2-dithiolato)vanadium, Inorg. Chem. 5 (1966) 411–416, https://doi.org/10.1021/ic50037a018.
- [31] R. Eisenberg, C.G. Pierpont, Trigonal-prismatic co-ordination. Crystal and molecular structure of tris-[cis-1,2-di(trifluoromethyl)ethylene-1,2-diselenato] molybdenum, J. Chem. Soc. A 14 (1971) 2285–2289, https://doi.org/10.1039/ 119710002285
- [32] D.G. VanDerveer, R. Eisenberg, Rhodium(I) dithiolene complexes. Synthesis, structure, and dynamic behavior, J. Am. Chem. Soc. 96 (1974) 4994–4996, https://doi.org/10.1021/ja00822a051.
- [33] J.A. Zuleta, J.M. Bevilacqua, D.M. Proserpio, P.D. Harvey, R. Eisenberg, Spectroscopic and theoretical studies on the excited state in diimine dithiolate complexes of platinum(II), Inorg. Chem. 31 (1992) 2396–2404, https://doi.org/ 10.1021/jc00038a019.
- [34] A.E. Smith, G.N. Schrauzer, V.P.H.W. Mayweg, The crystal and molecular structure of MoS6C6H6, J. Am. Chem. Soc. 87 (1965) 5798–5799, https://doi. org/10.1021/ia00952a054.
- [35] J.P. Donahue, C. Lorber, E. Nordlander, R.H. Holm, R.H., Molybdenum and tungsten structural analogues of the active sites of the MoIV + [O] → MoVIO oxygen atom transfer couple of DMSO reductases, J. Am. Chem. Soc. 120 (1998) 3259–3260, https://doi.org/10.1021/ja973917f.
- [36] K.B. Musgrave, J.P. Donahue, C. Lorber, R.H. Holm, B. Hedman, K.O. Hodgson, An X-ray spectroscopic investigation of bis(dithiolene)molybdenum(IV,V,VI) and -tungsten(IV,V,VI) complexes: symmetrized structural representations of the active sites of molybdoenzymes in the DMSO reductase family and of tungstoenzymes in the AOR and F(M)DH families, J. Am. Chem. Soc. 121 (1999) 10297–10307, https://doi.org/10.1021/ja990753p.
- [37] B.S. Lim, D.V. Fomitchev, R.H. Holm, Nickel dithiolenes revisited: structures and electron distribution from density functional theory for the three-member electron-tTransfer series [Ni(S2C2Me2)2]0,1-,2, Inorg. Chem. 40 (2001) 4257–4262. https://doi.org/10.1021/jc010138v.
- [38] F. Jalilehvand, B.S. Lim, R.H. Holm, B. Hedman, K.O. Hodgson, X-ray absorption spectroscopy of a structural analogue of the oxidized active sites in the sulfite oxidase enzyme family and related molybdenum(V) complexes, Inorg. Chem. 42 (2003) 5531–5536, https://doi.org/10.1021/ic030039f.
- [39] C.L. Beswick, J.M. Schulman, E.I. Stiefel, Structures and structural trends in homoleptic dithiolene complexes, Prog. Inorg. Chem. 52 (2003) 55–110, https://doi.org/10.1002/0471471933.ch2.
- [40] R.L. McNaughton, B.S. Lim, S.Z. Knottenbelt, R.H. Holm, M.L. Kirk, Spectroscopic and electronic structure studies of symmetrized models for reduced members of the dimethylsulfoxide reductase enzyme family, J. Am. Chem. Soc. 130 (2008) 4628–4636, https://doi.org/10.1021/ja074691b.
- [41] A.L. Tenderholt, R.K. Szilagyi, R.H. Holm, K.O. Hodgson, B. Hedman, E. I. Solomon, Electronic control of the "Bailar twist" in formally d0-d2 molybdenum tris(dithiolene) complexes: a sulfur K-edge x-ray absorption spectroscopy and density functional theory study, Inorg. Chem. 47 (2008) 6382–6392, https://doi.org/10.1021/ic800494h.
- [42] A.L. Tenderholt, J.-J. Wang, R.K. Szilagyi, R.H. Holm, K.O. Hodgson, B. Hedman, E.I. Solomon, Sulfur K-edge x-ray absorption spectroscopy and density functional calculations on Mo(IV) and Mo(VI)—O bis-dithiolenes: insights into the mechanism of oxo transfer in DMSO reductase and related functional analogues, J. Am. Chem. Soc. 132 (2010) 8359–8371, https://doi.org/10.1021/ja910369c.
- [43] G.P. Khare, R. Eisenberg, Synthesis and structure of the novel binuclear iridium-dithiolene complex dicarbonylbis(triphenylphosphine)tris(toluene-3,4-dithiolato)diiridium(III), Ir2(tdt)3(CO)2(P(C6H5)3)2, Inorg. Chem. 111(972) 1385–1392, https://doi.org/10.1021/ic50112a045.
- [44] B.S. Lim, J.P. Donahue, R.H. Holm, Synthesis and structures of bis(dithiolene) molybdenum complexes related to the active sites of the DMSO reductase enzyme family, Inorg. Chem. 39 (2000) 263–273, https://doi.org/10.1021/ic9908672.

- [45] B.S. Lim, K.-M. Sung, R.H. Holm, Structural and functional bis(dithiolene)-molybdenum/tungsten active site analogues of the dimethylsulfoxide reductase enzyme family, J. Am. Chem. Soc. 122 (2000) 7410–7411, https://doi.org/10.1021/ja001197y
- [46] J.H. Enemark, J.J.A. Cooney, J.-J. Wang, R.H. Holm, Synthetic analogues and reaction systems relevant to the molybdenum and tungsten oxotransferases, Chem. Rev. 104 (2004) 1175–1200, https://doi.org/10.1021/cr020609d.
- [47] R.H. Holm, E.I. Solomon, A. Majumdar, A. Tenderholt, Comparative molecular chemistry of molybdenum and tungsten and its relation to hydroxylase and oxotransferase enzymes, Coord. Chem. Rev. 255 (2011) 993–1015, https://doi. org/10.1016/j.ccr.2010.10.017.
- [48] E. Kianfar, M. Kaiser, G. Knor, Synthesis, characterization and photoreactivity of rhenium and molybdenum carbonyl complexes with iminopyridine ligands, J. Organomet. Chem. 799-800 (2015) 13–18, https://doi.org/10.1016/j. jorganchem.2015.08.015.
- [49] R.B. Ali, J. Burgess, M. Kotowski, R.V. Eldik, Solvent, ligand, pressure, and temperature effects on charge-transfer spectra of tetracarbonylmolybdenum(0) dimine complexes, Transit. Met. Chem. 12 (1987) 230–235, https://doi.org/ 10.1007/BE01023536
- [50] L.A. Garcia-Escudero, D. Miguel, J.A. Turiel, Carbonyl complexes of manganese, rhenium and molybdenum with ethynyliminopyridine ligands, J. Organomet. Chem. 691 (2006) 3434–3444, https://doi.org/10.1016/j. jorganchem.2006.04.024.
- [51] C.M. Alvarez, R. García-Rodríguez, D. Miguel, Carbonyl complexes of manganese, rhenium and molybdenum with 2-pyridylimino acid ligands, J. Organomet. Chem. 692 (2007) 5717–5726, https://doi.org/10.1016/j. iorganchem.2007.09.025.
- [52] C.M. Álvarez, R. García-Rodríguez, J.M. Martín-Alvarez, D. Miguel, Unexpected chemoselectivity in the Schiff condensation of amines with η2(C,O)- η1(O)coordinated aldehyde, Dalton Trans. 39 (2010) 1201–1203, https://doi.org/ 10.1039/B921892K.
- [53] C.M. Álvarez, R. García-Rodríguez, D. Miguel, Iminopyridine complexes of manganese, rhenium, and molybdenum derived from amino ester methylserine and peptides Gly-Gly, Gly-Val, and Gly-Gly-Gly: self-assembly of the peptide chains, Inorg. Chem. 51 (2012) 2984–2996, https://doi.org/10.1021/ic2022984.
- [54] R. Pal, T.L. Groy, R.J. Trovitch, Conversion of carbon dioxide to methanol using a C-H activated bis(imino)pyridine molybdenum hydroboration catalyst, Inorg. Chem. 54 (2015) 7506–7515, https://doi.org/10.1021/acs.inorgchem.5b01102.
- [55] R. Pal, J.A. Laureanti, T.L. Groy, A.K. Jones, R.J. Trovitch, Hydrogen production from water using a bis(imino)pyridine molybdenum electrocatalyst, Chem. Commun. 52 (2016) 11555–11558, https://doi.org/10.1039/C6CC04946J.
- [56] R. Pal, B. Cherry, M. Flores, T.L. Groy, R.J. Trovitch, Isolation of a bis(imino) pyridine molybdenum(I) iodide complex through controlled reduction and interconversion of its reaction products, Dalton Trans. 45 (2016) 10024–10033, https://doi.org/10.1039/C6DT00301J.
- [57] R. Pal, T.L. Groy, A.C. Bowman, R.J. Trovitch, Preparation and hydrosilylation activity of a molybdenum carbonyl complex that features a pentadentate bis (imino)pyridine ligand, Inorg. Chem. 53 (2014) 9357–9365, https://doi.org/ 10.1021/jc501465y.
- [58] G.W. Margulieux, S. Kim, P.J. Chirik, Determination of the N-H bond dissociation free energy in a pyridine(diimine)molybdenum complex prepared by protoncoupled electron transfer, Inorg. Chem. 59 (2020) 15394–15401, https://doi.org/ 10.1021/acs.inorgchem.0c02382.
- [59] G.W. Margulieux, Z.R. Turner, P.J. Chirik, Synthesis and ligand modification chemistry of a molybdenum dinitrogen complex: redox and chemical activity of a bis(imino)pyridine ligand, Angew. Chem. Int. Ed. 53 (2014) 14211–14215, https://doi.org/10.1002/ange.201408725.
- [60] M.J. Bezdek, P.J. Chirik, Pyridine(diimine) chelate hydrogenation in a molybdenum nitrido ethylene complex, Organometallics 38 (2019) 1682–1687, https://doi.org/10.1021/acs.organomet.9b00095.
- [61] G. Margulieux, M.J. Bezdek, Z.R. Turner, P.J. Chirik, Ammonia activation, H2 evolution and nitride formation from a molybdenum complex with a chemically and redox noninnocent ligand, J. Am. Chem. Soc. 139 (2017) 6110–6113, https://doi.org/10.1021/jacs.7b03070.
- [62] A. Bheemaraju, R.L. Lord, P. Müller, S. Groysman, Difference in the reactivities of H- and Me-substituted dinucleating bis(iminopyridine) ligands with nickel(0), Organometallics 31 (2012) 2120–2123, https://doi.org/10.1021/om300067z.
- [63] A. Bheemaraju, J.W. Beattie, E.G. Tabasan, P.D. Martin, R.L. Lord, S. Groysman, Steric and electronic effects in the formation and carbon disulfide reactivity of dinuclear nickel complexes supported by bis(iminopyridine) ligands, Organometallics 32 (2013) 2952–2962, https://doi.org/10.1021/om400187v.
- [64] A. Bheemaraju, J.W. Beattie, R.L. Lord, P.D. Martin, S. Groysman, Carbon disulfide binding at dinuclear and mononuclear nickel complexes ligated by a redox-active ligand: iminopyridine serving as an accumulator of redox equivalents for the activation of heteroallenes, Chem. Commun. 48 (2012) 9595–9597, https://doi.org/10.1039/C2CC34307J.
- [65] B.R. Reed, S.A. Stoian, R.L. Lord, S. Groysman, The aldimine effect in bis(imino) pyridine complexes: non-planar nickel(I) complexes of a bis(aldimino)pyridine ligand, Chem. Commun. 51 (2015) 6496–6499, https://doi.org/10.1039/C5CC00203F.
- [66] B.R. Reed, M. Yousif, R.L. Lord, M. McKinnon, J. Rochford, S. Groysman, Coordination chemistry and reactivity of bis(aldimino) pyridine nickel complexes in four different oxidation states, Organometallics 36 (2017) 582–593, https:// doi.org/10.1021/acs.organomet.6b00793.
- [67] R. Narayanan, M. McKinnon, B.R. Reed, K.T. Ngo, S. Groysman, J. Rochford, Ambiguous electrocatalytic CO2 reduction behavior of a nickel bis (aldimino)

- pyridine pincer complex, Dalton Trans. 45 (2016) 15285–15289, https://doi.org/
- [68] R.L. Hollingsworth, A. Bheemaraju, N. Lenca, R.L. Lord, S. Groysman, Divergent reactivity of a new dinuclear xanthene-bridged bis (iminopyridine) di-nickel complex with alkynes, Dalton Trans. 46 (2017) 5605–5616, https://doi.org/ 10.1039/C6DT04532D.
- [69] R.L. Hollingsworth, J.W. Beattie, A. Grass, P.D. Martin, S. Groysman, R.L. Lord, Reactions of dicobalt octacarbonyl with dinucleating and mononucleating bis (imino) pyridine ligands, Dalton Trans. 47 (2018) 15353–15363, https://doi.org/ 10.1039/C8DT03405B.
- [70] Gaussian O9, Revision D.01, M.J. Frisch, G.W. Trucks, H.B. Schlegel, G. E. Scuseria, M.A. Robb, J.R. Cheeseman, G. Scalmani, V. Barone, G.A. Petersson, H. Nakatsuji, X. Li, M. Caricato, A. Marenich, J. Bloino, B.G. Janesko, R. Gomperts, B. Mennucci, H.P. Hratchian, J.V. Ortiz, A.F. Izmaylov, J. L. Sonnenberg, D. Williams-Young, F. Ding, F. Lipparini, F. Egidi, J. Goings, B. Peng, A. Petrone, T. Henderson, D. Ranasinghe, V.G. Zakrzewski, J. Gao, N. Rega, G. Zheng, W. Liang, M. Hada, M. Ehara, K. Toyota, R. Fukuda, J. Hasegawa, M. Ishida, T. Nakajima, Y. Honda, O. Kitao, H. Nakai, T. Vreven, K. Throssell, J.A. Montgomery Jr., J.E. Peralta, F. Ogliaro, M. Bearpark, J.J. Heyd, E. Brothers, K.N. Kudin, V.N. Staroverov, T. Keith, R. Kobayashi, J. Normand, K. Raghavachari, A. Rendell, J.C. Burant, S.S. Iyengar, J. Tomasi, M. Cossi, J. M. Millam, M. Klene, C. Adamo, R. Cammi, J.W. Ochterski, R.L. Martin, K. Morokuma, O. Farkas, J.B. Foresman, D.J. Fox, Gaussian, Inc., Wallingford CT, 2016.
- [71] Gaussian 16, Revision B.01, M.J. Frisch, G.W. Trucks, H.B. Schlegel, G. E. Scuseria, M.A. Robb, J.R. Cheeseman, G. Scalmani, V. Barone, G.A. Petersson, H. Nakatsuji, X. Li, M. Caricato, A.V. Marenich, J. Bloino, B.G. Janesko, R. Gomperts, B. Mennucci, H.P. Hratchian, J.V. Ortiz, A.F. Izmaylov, J. L. Sonnenberg, D. Williams-Young, F. Ding, F. Lipparini, F. Egidi, J. Goings, B. Peng, A. Petrone, T. Henderson, D. Ranasinghe, V.G. Zakrzewski, J. Gao, N. Rega, G. Zheng, W. Liang, M. Hada, M. Ehara, K. Toyota, R. Fukuda, J. Hasegawa, M. Ishida, T. Nakajima, Y. Honda, O. Kitao, H. Nakai, T. Vreven, K. Throssell, J.A. Montgomery Jr., J.E. Peralta, F. Ogliaro, M.J. Bearpark, J. J. Heyd, E.N. Brothers, K.N. Kudin, V.N. Staroverov, T.A. Keith, R. Kobayashi, J. Normand, K. Raghavachari, A.P. Rendell, J.C. Burant, S.S. Iyengar, J. Tomasi, M. Cossi, J.M. Millam, M. Klene, C. Adamo, R. Cammi, J.W. Ochterski, R. L. Martin, K. Morokuma, O. Farkas, J.B. Foresman, D.J. Fox, Gaussian, Inc., Wallingford CT, 2016.
- [72] A.D. Becke, Density-functional exchange-energy approximation with correct asymptotic behavior, Phys. Rev. A 38 (1988) 3098–3100, https://doi.org/ 10.1103/PhysRevA.38.3098.
- [73] J.P. Perdew, Density-functional approximation for the correlation energy of the inhomogeneous electron gas, Phys. Rev. B 33 (1986) 8822–8824, https://doi.org/ 10.1103/PhysRevB.33.8822.
- [74] F. Weigend, R. Ahlrichs, Balanced basis sets of split valence, triple zeta valence and quadruple zeta valence quality for H to Rn: design and assessment of accuracy, Phys. Chem. Chem. Phys. 7 (2005) 3297–3305, https://doi.org/ 10.1039/B508541A
- [75] F. Weigend, Accurate Coloumb-fitting basis sets for H to Rn, Phys. Chem. Chem. Phys. 8 (2006) 1057–1065, https://doi.org/10.1039/BH15623H.
- [76] A.N. Bootsma, S.E. Wheeler, Popular integration grids can result in large errors in DFT-computed free energies. ChemRxiv, Preprint, 10.26434/chemrxiv.8864204. v5.
- [77] H.B. Schlegel, Geometry optimization, WIREs Comput. Mol. Sci. 1 (2011) 790–809, https://doi.org/10.1002/wcms.34.
- [78] J.L. Sonnenberg, H.B. Schlegel, H.P. Hratchian, Spin contamination in inorganic chemistry calculations, in: E.I. Solomon, R.B. King, R.A. Scott (Eds.), Computational Inorganic and Bioinorganic Chemistry, Wiley, Chichester, U.K, 2009, pp. 173–186, https://doi.org/10.1002/0470862106.ia617.
- [79] S.H. Vosko, L. Wilk, M. Nusair, Accurate spin-dependent electron liquid correlation energies for local spin density calculations: a critical analysis, Can. J. Phys. 58 (1980) 1200–1211, https://doi.org/10.1139/p80-159.
- [80] C. Lee, W. Yang, R.G. Parr, Development of the Colle-Salvetti correlation-energy formula into a functional of the electron density, Phys. Rev. B 37 (1988) 785–789, https://doi.org/10.1103/PhysRevB.37.785.
- [81] A.D. Becke, Density-functional thermochemistry. III. The role of exact exchange, J. Chem. Phys. 98 (1993) 5648–5652, https://doi.org/10.1063/1.464913.
- [82] P.J. Stephens, F.J. Devlin, C.F. Chabalowski, M.J. Frisch, Ab initio calculation of vibrational absorption and circular dichroism spectra using density functional force fields, J. Phys. Chem. 98 (1994) 11623–11627, https://doi.org/10.1021/ j100096a001.
- [83] A.V. Marenich, C.J. Cramer, D.G. Truhlar, Universal solvation model based on solute electron density and on a continuum model of the solvent defined by the bulk dielectric constant and atomic surface tensions, J. Phys. Chem. B 113 (2009) 6378–6396, https://doi.org/10.1021/jp810292n.
- [84] G. Scalmani, M.J. Frisch, B. Mennucci, J. Tomasi, R. Cammi, V. Barone, Geometries and properties of excited states in the gas phase and in solution: theory and application of a time-dependent density functional theory polarizable continuum model, J. Chem. Phys. 124 (094107) (2006) 1–15, https://doi.org/ 10.1062 (1.2173258)
- [85] T. Yanai, D. Tew, N. Handy, A new hybrid exchange-correlation functional using the Coulomb-attenuating method (CAM-B3LYP), Chem. Phys. Lett. 393 (2004) 51–57, https://doi.org/10.1016/j.cplett.2004.06.011.
- [86] R. Balamurugan, M. Palaniandavar, M.A. Halcrow, Copper (II) complexes of sterically hindered Schiff base ligands: synthesis, structure, spectra and

- electrochemistry, Polyhedron 25 (2006) 1077–1088, https://doi.org/10.1016/j.poly.2005.07.047.
- [87] D.P. Tate, W.R. Knipple, J.M. Augl, Nitrile derivatives of chromium group metal carbonyls, Inorg. Chem. 1 (1962) 433–434, https://doi.org/10.1021/ ic50002a052.
- [88] B.L. Ross, J.G. Grasselli, W.M. Ritchey, H.D. Kaesz, Spectroscopic studies of the complexes of acrylonitrile and acetonitrile with the carbonyls of chromium, molybdenum, and tungsten, Inorg. Chem. 2 (1963) 1023–1030, https://doi.org/ 10.1021/ic50009a034.
- [89] W. Hieber, A. Lipp, Reaktionen der Eisencarbonyle mit verschiedenartigen Basen, IV. Umsetzungen mit Pyridin N-oxyd, Dimethylsulfoxyd, Triphenylphosphinoxyd u. ä, Chem. Ber. 92 (1959) 2085–2088, https://doi.org/10.1002/ cher.1959020019
- [90] Y. Shvo, E.A. Hazum, A new method for the synthesis of organic iron carbonyl complexes, J. Chem. Soc. Chem. Commun. 20 (1975) 829–830, https://doi.org/ 10.1039/C39750000829.
- [91] Y.L. Shi, Y.C. Gao, Q.Z. Shi, D.L. Kershner, F. Basolo, Oxygen atom transfer reactions to metal carbonyls. Kinetics and mechanism of carbon monoxide substitution reactions of M(CO)6 (M = chromium, molybdenum, tungsten) in the presence of trimethylamine oxide, Organometallics 6 (1987) 1528–1531, https:// doi.org/10.1021/om00150a027.
- [92] J.-K. Shen, Y.-C. Gao, Q.-Z. Shi, F. Basolo, Oxygen-atom-transfer reactions to metal carbonyls. Kinetics and mechanism of CO substitution of M (CO) 5 (M= Fe, Ru, Os) in the presence of trimethylamine oxide, Organometallics 8 (1989) 2144–2147, https://doi.org/10.1021/om00111a008.
- [93] A.M. Kelly, G.P. Rosini, A.S. Goldman, Oxygen transfer from organoelement oxides to carbon monoxide catalyzed by transition metal carbonyls, J. Am. Chem. Soc, 119 (1997) 6115–6125, https://doi.org/10.1021/ja970158s.
- [94] S. Dilsky, Molybdenum and tungsten complexes of the neutral tripod ligands HC (pz)3 and MeC(CH2PPh2)3, J. Organomet. Chem. 692 (2007) 2887–2896, https://doi.org/10.1016/j.jorganchem.2007.02.021.
- [95] P.K. Baker, S.G. Fraser, E.M. Keys, The synthesis and spectral properties of some highly reactive new seven-coordinate molybdenum (II) and tungsten (II) bisacetonitrile dihalogenotricarbonyl complexes, J. Organomet. Chem. 309 (1986) 319–321, https://doi.org/10.1016/S0022-328X(00)99633-5.
- [96] P. Chaudhuri, K. Wieghardt, Y.H. Tsai, C. Krüger, Reactions of LM(CO)3 complexes (M= Cr, Mo, W; L= 1, 4, 7-triazacyclononane) with bromine, iodine, and nitric acid. Syntheses of air-stable hydridocarbonyl and hydridonitrosyl complexes. Crystal structure of [LMo(CO)3Br](ClO4). H2O, Inorg. Chem. 23 (1984) 427-432, https://doi.org/10.1021/ic00172a010.
- [97] M.D. Curtis, K. Shiu, Synthesis, structure, and fluxional behavior of 7-coordinate complexes: TpMo(CO)3X (X= H, Br, I; Tp= hydridotripyrazolylborato), Inorg. Chem. 24 (1985) 1213–1218, https://doi.org/10.1021/ic00202a020.
- [98] S.J. Coles, P.G. Edwards, J.S. Fleming, M.B. Hursthouse, Triphosphorus macrocycle complexes of divalent Group 6 transition metals; crystal structure of bromotricarbonyl-[1, 5, 9-tris (isopropyl)-1, 5, 9-triphosphacyclododecane]-molybdenum (II) tetraphenylborate, J. Chem. Soc., Dalton Trans. 24 (1995) 4091–4097. https://doi.org/10.1039/DT9950004091.
- [99] R. Pal, T.L. Groy, R.J. Trovitch, Conversion of carbon dioxide to methanol using a C-H activated bis (imino) pyridine molybdenum hydroboration catalyst, Inorg. Chem. 54 (2015) 7506–7515, https://doi.org/10.1021/acs.inorgchem.5b01102.
- [100] S.R.M.M. de Aguiar, B. Stöger, E. Pittenauer, G. Allmaier, L.F. Veiros, K. Kirchner, Structural diversity of halocarbonyl molybdenum and tungsten PNP pincer complexes through ligand modifications, Dalton Trans. 45 (2016) 13834–13845, https://doi.org/10.1039/C6DT02251K.
- [101] P. Planinic, H. Meider, Carbonyl and halocarbonyl complexes of molybdenum and tungsten with oxygen donor ligands, Polyhedron 9 (1990) 1099–1105, https:// doi.org/10.1016/S0277-5387(00)81301-7.
- [102] D. Benito-Garagorri, E. Becker, J. Wiedermann, W. Lackner, M. Pollak, K. Mereiter, J. Kisala, K. Kirchner, Achiral and chiral transition metal complexes with modularly designed tridentate PNP pincer-type ligands based on Nheterocyclic diamines, Organometallics 25 (2006) 1900–1913, https://doi.org/ 10.1021/om0600644.
- [103] T. Vielhaber, K. Faust, C. Topf, Group 6 metal carbonyl complexes supported by a bidentate PN ligand: syntheses, characterization, and catalytic hydrogenation activity, Organometallics 39 (2020) 4535–4543, https://doi.org/10.1021/acs. organomet.0c00612.
- [104] T.S. Hollingsworth, R.L. Hollingsworth, T. Rosen, S. Groysman, Zinc bimetallics supported by a xanthene-bridged dinucleating ligand: synthesis, characterization, and lactide polymerization studies, RSC Adv. 7 (2017) 41819–41829, https://doi. org/10.1039/C7RA09207E.
- [105] T. Jurca, W.-C. Chen, S. Michel, I. Korobkov, T.-G. Ong, D.S. Richeson, Solid-state thermolysis of a fac-rhenium(I) carbonyl complex with a redox non-innocent pincer ligand, Chem. Eur. J. 19 (2013) 4278–4286, https://doi.org/10.1002/ chem.201203045.
- [106] N. Cosquer, B. Le Gall, F. Conan, J.-M. Kerbaol, J. Sala-Pala, M.M. Kubicki, E. Vigier, Carbonylmolybdenum complexes with di(imino)pyridine and related ligands: reduction of a di(imino)pyridine to an aminoiminopyridine system under mild conditions, Inorg. Chim. Acta 359 (2006) 4311–4316, https://doi.org/ 10.1016/j.ica.2006.06.005.
- [107] A.Z. Spentzos, M.R. Gau, P.J. Carroll, N.C. Tomson, Unusual cyanide and methyl binding modes at a dicobalt macrocycle following acetonitrile C–C bond activation, Chem. Commun. 56 (2020) 9675–9678, https://doi.org/10.1039/ DOCC03521A.
- [108] Q. Wang, S. Zhang, P. Cui, A.B. Weberg, L.M. Thierer, B.C. Manor, M.R. Gau, P. J. Carroll, N.C. Tomson, Interdependent metal-metal bonding and ligand redox-

- activity in a series of dinuclear macrocyclic complexes of iron, cobalt, and nickel, Inorg. Chem. 59 (2020) 4200–4214, https://doi.org/10.1021/acs.
- [109] E.D. Reinhart, R.F. Jordan, Template-free synthesis of a macrocyclic bis(pyridine-dienamine) proligand and metal complexes of its bis(pyridine-diimine) and bis (pyridine-dienamido) forms, Inorg. Chem. 58 (2019) 15466–15478, https://doi.org/10.1021/acs.inorgchem.9b02539.
- [110] E.D. Reinhart, R.F. Jordan, Synthesis and ethylene reactivity of dinuclear iron and cobalt complexes supported by macrocyclic bis(pyridine-diimine) ligands containing o-terphenyl linkers, Organometallics 39 (2020) 2392–2404, https:// doi.org/10.1021/acs.organomet.0c00211.
- [111] H. Vazquez-Lima, J. Conradie, M.A.L. Johansen, S.R. Martinsen, A.B. Alemayehu, A. Ghosh, Heavy-element-ligand covalence: ligand noninnocence in molybdenum and tungsten Viking-helmet Corroles, Dalton Trans. 50 (2021) 12843–12849, https://doi.org/10.1039/D1DT01970H.
- [112] S. Ganguly, A. Ghosh, Seven clues to ligand noninnocence: the metallocorrole paradigm, Acc. Chem. Res. 52 (7) (2019) 2003–2014, https://doi.org/10.1021/ acs.accounts.9b00115.
- [113] G. Parkin, Valence, oxidation number, and formal charge: three related but fundamentally different concepts, J. Chem. Educ. 83 (2006) 791–799, https:// doi.org/10.1021/ed083p791.